MONTANA STATE UNIVERSITY

Boiling heat transfer characteristics of several organic liquids
by Lloyd Grainger Becraft

A thesis submitted to the Graduate Faculty in partial fulfillment of the requirements for the degree of
DOCTOR OF PHILOSOPHY in Chemical Engineering
Montana State University
© Copyright by Lloyd Grainger Becraft (1962)

Abstract:
Interest in high heat transfer rates has brought about increased interest in boiling heat transfer — a method of attaining high heat fluxes. This research project was designed to investigate the effect of liquid properties on boiling heat transfer rates, keeping the heat transfer surface constant. The liquids studied were carbon tetrachloride, chloroform, 1, 1, 1-trichloroethane, benzene, cyclohexane, ethyl acetate, ethylene dichloride, and trichloroethylene.

The total heat flux was found to be proprotional to N^a where N was the active nucleate site population and a had a value between one-half and one. This value of a was dependent on the liquid under study and the population of sites.

The nucleate heat transfer rate (Q_n) per bubble site varied with the liquid studied. Those liquids with steep boiling curves tended to have a constant-heat transfer rate per site. Liquids with boiling curves (Q/A versus Tx, where Tx equals temperature of heating surface minus temperature of saturation) of smaller slope had higher heat transfer rates per site as the number of sites increased. Higher rates per site occurred with liquids which started nucleate boiling at higher temperature excesses (Tx's). This indicates the heat transfer rate per nucleate site was highly dependent on the heat transfer surface.

The theory of multiple linear regression was applied to develop a correlation for the heat flux during nucleate boiling. The variables listed in order of decreasing importance were.; temperature excess, liquid viscosity, heat capacity of the liquid, liquid density, temperature of heating surface, thermal conductivity of the liquid, latent heat of vaporization, vapor density, and surface tension.

BOILING HEAT TRANSFER CHARACTERISTICS
OF SEVERAL ORGANIC LIQUIDS

by

LLOYD G. BECRAFT   1936 -

A thesis submitted to the Graduate Faculty in partial
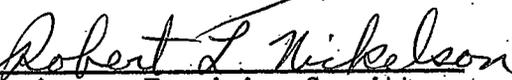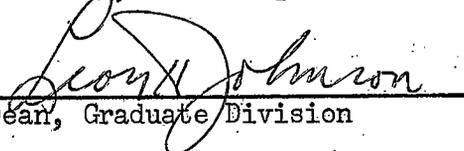fulfillment of the requirements for the degree

of

DOCTOR OF PHILOSOPHY

in

Chemical Engineering

Approved:

[signature: Lloyd Berg]

Head, Major Department

[signature: Robert L. Nickelson]

Chairman, Examining Committee

[signature: Leon H. Johnson]

Dean, Graduate Division

MONTANA STATE COLLEGE
Bozeman, Montana

August, 1962

ii

VITA

The author, Lloyd Grainger Becraft, was born April 5, 1936, in Glasgow, Montana, the son of Edwin R. Becraft (B.S. Ch.E., Montana State College, 1932) and Gladys G. Becraft. He attended Central High School in La Crosse, Wisconsin, St. Louis Park High School, St. Louis Park, Minnesota, and graduated from Billings Senior High School, Billings, Montana, in June, 1954. In June, 1958, he graduated from Montana State College with a Bachelor of Science in Chemical Engineering.

His experience includes the following:

Technologist, Shell Chemical Corporation, Torrance, California, June, 1957, to September, 1957

Reservoir Engineer, Shell Oil Company, Billings, Montana, June, 1958, to September, 1958

Research Fellow in Chemical Engineering, Montana State College, Bozeman, Montana, October, 1958, to December, 1961

Graduate Assistant in Mathematics, Montana State College, Bozeman, Montana, September, 1958, to June, 1960, and September, 1961, to December, 1961.

He is presently employed as a Research Chemical Engineer with the Process Laboratory, Research and Development Department, Continental Oil Company, Ponca City, Oklahoma.

He and his wife, Dianne, and daughter, Wanda, now reside in Ponca City, Oklahoma.

ACKNOWLEDGMENT

TABLE OF CONTENTS

v

LIST OF TABLES

vi

LIST OF FIGURES

ABSTRACT

Interest in high heat transfer rates has brought about increased interest in boiling heat transfer -- a method of attaining high heat fluxes. This research project was designed to investigate the effect of liquid properties on boiling heat transfer rates, keeping the heat transfer surface constant. The liquids studied were carbon tetrachloride, chloroform, 1, 1, 1-trichloroethane, benzene, cyclohexane, ethyl acetate, ethylene dichloride, and trichloroethylene.

The total heat flux was found to be proprotional to N^a where N was the active nucleate site population and a had a value between one-half and one. This value of a was dependent on the liquid under study and the population of sites.

The nucleate heat transfer rate (Q_n) per bubble site varied with the liquid studied. Those liquids with steep boiling curves tended to have a constant heat transfer rate per site. Liquids with boiling curves (Q/A versus T_x, where T_x equals temperature of heating surface minus temperature of saturation) of smaller slope had higher heat transfer rates per site as the number of sites increased. Higher rates per site occurred with liquids which started nucleate boiling at higher temperature excesses (T_x's). This indicates the heat transfer rate per nucleate site was highly dependent on the heat transfer surface.

The theory of multiple linear regression was applied to develop a correlation for the heat flux during nucleate boiling. The variables listed in order of decreasing importance were: temperature excess, liquid viscosity, heat capacity of the liquid, liquid density, temperature of heating surface, thermal conductivity of the liquid, latent heat of vaporization, vapor density, and surface tension.

I. INTRODUCTION

The advent of rocket engines, nuclear reactors, and manned space cap-
sules has caused increased interest in boiling heat transfer. Boiling liq-
uids can transfer heat at rates much greater than those obtained by convec-
tion, conduction or radiation. Industrial heat exchangers operate at 500
to 50,000 Btu/hr-ft^2; boiling water in vortex flow has transferred heat at
rates up to 35,000,000 Btu/hr-ft^2 (2). This approaches the 45,000,000 es-
timated for satellite re-entry.

Intelligent design of heat-transfer equipment requires a thorough
knowledge of the mode of transfer involved. Until recently boiling heat
transfer theory was scarce. However, the past decade has seen many attempts
to fill this knowledge gap (20,21,22). This research investigated one type
of boiling heat transfer—nucleate pool boiling. The ultimate aim was to
eliminate the effect of different surfaces on the boiling heat flux and
study only the effect of liquid properties on the flux. Liquids investi-
gated were carbon tetrachloride, chloroform, 1, 1, 1-trichloroethane,
benzene, cyclohexane, ethyl acetate, ethylene dichloride, and trichloroeth-
ylene. The heat transfer surface was an electrically-heated gold or cop-
per wire. Heat fluxes were generally held to the ranges in which nucleate
boiling sites could be counted visually.

II. EXPERIMENTAL CONSIDERATIONS

Equipment

The experiments in this investigation were carried out in a glass system closed to the atmosphere. The system pressure could be controlled easily from slightly under atmospheric pressure to 760 mm of mercury by means of a pressure control bulb. The heat transfer surface was an electrically-heated wire immersed in the liquid under study. Measurement of the current passing through the wire, the resistance of the wire, and the surface area of the wire permitted the calculation of the heat flux (Q/A). The average temperature of the wire was obtained by the use of the wire as a resistance thermometer.

Figure 1 presents a simplified schematic diagram of the experimental setup. A Pyrex kettle, $5\frac{1}{4}$ inches in diameter and 7 inches deep, served as the boiler for this investigation. The lid was mounted firmly to the support rack by a suspension system of stainless steel tubing which entered the lid through a hole in the center and formed a circular support system on the underside of the lid. The kettle itself was held to the lid by a clamp which encircled the flanges of the lid and kettle. This setup allowed the removal of the kettle to change liquids or boiling wires without disassembling the entire system or breaking glass seals.

Two $\frac{1}{2}$-inch copper rods passed through the lid into the liquid. These rods were permanently attached to the glass lid by ordinary corks sealed with Epon resin on the outside. A glass tube with a standard taper joint fit into a third hole in the lid. Fisher Non-aqueous Stopcock Grease

was used to help seal this ground-glass joint as well as the ground-glass
flange between the lid and the kettle. The glass tube led to the pressure-
control bulb. More glass tubing led from this bulb to an open-end mercury
manometer (See Fig. 1).

The pressure-control bulb was a modified round-bottom flask attached
at right angles to the top of the condenser. Two copper wires entered the
neck of the flask through metal-to-glass seals. These wires conducted
electric current to a bare wire Nichrome coil immersed in the liquid in the
bulb. Varying the power to the coil controlled the pressure in the system.
This power was controlled in two ways. The current first passed through
a conventional Variac. A variable resistance was thrown in and out of the
circuit between the Variac and heating coil by an electronic relay. In-
creasing pressure in the system caused the mercury in the manometer to
rise in the open-end leg. When this mercury touched a preset contact in
the leg, the completed circuit in the electronic relay operated another re-
lay. Current flowed through this second relay from the Variac through a
variable resistance to the pressure controller. Setting the contact at
different positions in the leg of the manometer fixed the pressure in the
system. If the pressure had a tendency to surpass the set point, two
coarse controls were employed. The setting on the Variac in line with the
pressure controller was lowered, and/or air was blown across the glass tub-
ing above the boiler by means of a small electric fan.

The pressure control bulb was insulated with glass wool covered with
aluminum foil. During experimental runs, the boiler was enclosed in an
insulating box of Celotex fastened in a rectangular 5-gallon metal container.

A small glass window in the side of this box allowed visual observation of the boiling surface. A small electric bulb in the box provided excellent visibility. An electrically-heated Nichrome wire inside the box furnished enough heat to keep the liquid in the boiler at the appropriate boiling temperature.

The heat transfer surface, a 20-gauge gold or copper wire, was clamped to the two $\frac{1}{2}$-inch copper rods inside the boiler. On this horizontal wire were silver-soldered two 30-gauge copper wires which served as potential leads. These leads were clamped to 20-gauge copper wires leading out of the boiler through a cork in the lid. In addition to these wires, the two stainless steel support rods and a 12-gauge copper wire also entered the boiler through this cork. The cork was sealed with Epon resin on the outside.

In the bottom of the boiler was a coil of Nichrome wire which served as an auxiliary heater for degassing the liquid. This coil was fastened between the 12-gauge copper wire and one $\frac{1}{2}$-inch copper rod inside the boiler. A Variac controlled the amount of current sent to this heater.

A 3-KVA motor-generator supplied direct current at 6-9 volts for heating the experimental boiling surface--the 20-gauge gold or copper wire. The power output of the generator was controlled by varying the field current. The direct current for this separately excited field came from a rectifying bridge made from silicon rectifiers. This bridge was in turn supplied with alternating current from a 220-volt Variac. For better control a resistance was placed in series with the boiling wire. This consisted of a bare wire copper coil immersed in a polyethylene bucket through

which water flowed continuously.

A Brown potentiometer indicated the voltage drop across a precision shunt in series with the boiling wire, the wire from which boiling took place. From this the current passing through the wire could be calculated. The resistance of the test section of the wire (that between the potential leads) was measured with a Kelvin double bridge. The precision shunt mentioned previously could be brought into the Kelvin bridge circuit as a known resistance with a knife-blade double-throw switch. Two 500-ohm precision resistances and two General Radio decade resistance boxes completed the bridge circuit. The resistance of the wire test section could be determined from the decade box readings when the Leeds and Northrup K-3 galvanometer showed that the bridge was balanced. Another double-throw knife-blade switch was used to reverse the leads to the galvanometer. This increased the accuracy of determining the null point.

Procedure

One of the important variables in heat transfer is the temperature of the heat source. The temperature of the boiling wire in this study was found by using the center section as a resistance thermometer. Knowing the resistance of this section from the balancing of the Kelvin bridge, the average temperature was obtained from a calibration curve of temperature versus resistance. This calibration curve was obtained before the experimental runs with the help of a constant temperature oil bath. An ordinary 12-volt lead storage battery supplied the small amount of direct current used in the calibration. At each of the temperatures, resistance readings were taken for several different amperages. A variable resistance between

the battery and boiling wire controlled these currents. A plot of resistance versus the square of the amperage was linear and could be extrapolated back to zero amperes. These intercepts were the values used in the calibration curves.

Before each run the boiling wire was thoroughly cleaned in acetone and clamped between the $\frac{1}{2}$-inch copper rods. The potential leads were then attached to the 20-gauge copper wires leading out of the boiler. The boiler was cleaned with hot water and scouring cleanser, then rinsed with hot tap water followed by a thorough acetone wash. The appropriate liquid was added to the boiler, the glass flanges were greased, and the boiler was clamped to the lid. The copper rods and other equipment hanging below the lid were rinsed in acetone before the boiler was put in place.

The Nichrome coil brought the liquid to boiling. Eventually the pressure-control bulb and inner leg of the manometer filled with the liquid. Permanent gases were released from the system by opening the Teflon stopcock above the inner leg of the manometer. The liquid boiled for 24 hours at a pressure slightly above atmospheric (about 640 mm. at Bozeman, Montana) during this degassing period. Just before the experimental run, the pressure in the system was raised to 760 millimeters of mercury by raising the contact in the open leg of the manometer to the appropriate height. This height had to be calculated from knowledge of the atmospheric pressure and the pressure exerted by the liquid column in the inner leg of the manometer.

The auxiliary heater was turned off and direct current from the generator was used to heat the boiling wire. The power was increased slowly,

stopping at intervals to record the resistance of the wire and the amount of current passing through it. When boiling started on the wire, the power was increased until the wire was covered evenly with nucleate boiling sites. The power was then decreased in small intervals. At each stopping point the resistance of the wire, the current flowing through it, and the number of nucleate boiling sites between the potential lead contacts were recorded.

III. THEORY

Fundamental research into the phenomenon of boiling heat transfer be-
gan with Nukiyama's study in 1934 (17). He used an electrically-heated
horizontal wire immersed in water, a simple method still used today.

Boiling curves, as first described by Nukiyama, are similar for all
liquids (see Fig. 2). When the temperature of the heating surface (T_w)
becomes greater than the saturation temperature (T_s) of the liquid, heat
transfers by natural convection. As the difference between the tempera-
ture of the heating surface and the temperature of saturation (tempera-
ture excess, T_x) increases, boiling starts at discrete points on the hot
surface. This is the region of nucleate boiling. The curve rises to a
maximum known as the burnout point. This name evolved from the fact that
a wire made from a low-melting metal will melt at this point when it is
used as an electrically-heated surface for boiling experiments. A region
of strange behavior called the transition region follows the burnout point
with increasing temperature excess. Here, for an increase in temperature
excess, the heat flux decreases. No solid-liquid contact exists. The
heating surface is covered with an uneven, unstable vapor blanket. This
vapor blanket stabilizes and releases "globs" of vapor in a regular manner
when boiling reaches the next region, film boiling. Once film boiling
starts, the heat flux again increases with increasing temperature excess.

Several mechanisms have been proposed (7) to explain the high heat
fluxes obtained in boiling. The commonly accepted theory is that the
bubble growth and release induces a form of micro-convention in the

normally laminar sublayer. These bubble growth rates could cause radial liquid velocities in the order of 10-20 ft/sec. The Sieder-Tate convective heat transfer equation (See Ref. 13, p. 544,47) predicts the order of magnitude of the observed heat flux when these velocities are used in the Reynolds number term. However, this equation is only recommended for turbulent flow across the heating surface. The temperature distribution near the heating surface is probably quite different for bubble-induced random velocities and steady flow conditions.

The main argument against this theory comes from the experimental evidence indicating that the heat flux is dependent on the temperature excess ($T_{wall} - T_{sat}$) rather than temperature difference, $T_{wall} - T_{liquid}$. For the same T_x ($T_w - T_s$) the heat flux remains essentially the same regardless of the subcooling of the liquid (14).

Perhaps the first mechanism one would think of to explain the heat transfer in a boiling liquid would be simple latent heat transport by the bubbles. The heat emitted from the source is absorbed by the growing bubble as latent heat of vaporization. The theory appears intuitively sound, but experimental findings do not verify it. Forster and Greif (7) have used the data of Gunther and Kreith (10) for subcooled boiling in water to cast considerable doubt on the validity of this mechanism. Their presentation is as follows:

observed heat flux $\frac{Q}{A} = 2.0$ BTU/(sec)(in)^2

maximum bubble radius $R = 0.015$ in

frequency of bubble cycle $f = 1000$/sec

bubble population $N = 280$/in^2

latent heat delivered to bulk liquid per bubble

$$\lambda \rho_v V_B = (970 \text{ BTU/lb})(2 \times 10^{-5} \text{ lb/in}^3)(7 \times 10^{-6} \text{ in}^3) = 1.4 \times 10^{-7} \text{ BTU/bubble}$$

total latent heat transport

$$(1.4 \times 10^{-7} \text{ BTU/bubble})(280)(1000) = 0.04 \text{ BTU/(sec)(in)}^2$$

This result is only 2% of the total heat flux.

One factor has been ignored in this mechanism -- the possibility of more heat transfer through the bubble by mass transfer.

Another possible mechanism is a vapor - liquid exchange action. When a bubble grows and detaches or collapses (as often is the case in subcooled boiling), a quantity of hot liquid is pushed away from the heat source into the bulk of the liquid. If this were a perfect exchange, the ratio of heat transferred by the action to that transferred by the latent heat mechanism would be expressed by

$$(1.) \qquad M = -\frac{C_L \rho_L \Delta T_{MEAN}}{\lambda \rho_v}$$

The T_{mean} represents the difference between the heat contents of a sphere of hot liquid and one of liquid at the bulk temperature. Since there is a temperature gradient in the liquid from the hot surface to the bulk liquid, the sphere of hot liquid is considered to be at some temperature intermediate between T_{wall} and T_{liquid} -- thus, the use of a mean ΔT.

The ratio ρ_L/ρ_v is large enough to offset the magnitude of the latent heat λ. For water at atmospheric pressure, $M = 1.7 \Delta T_{mean}$. The data from Gunther and Kreith gives an approximation for the ratio M. In one experiment they measured both the bubble radii and the temperature profile in the liquid near the heat source. From their measurements ΔT_{mean} is approximately 95°F. The ratio M then becomes 160 which means the heat

transferred by a perfect exchange of hot liquid for cool is 160 times that transferred by the latent heat mechanism. Since latent heat transport accounted for 2% of the total heat flux, this exchange could account for well over the observed value of heat transfer. Practically, the heat flux would never reach the theoretical maximum since a complete exchange of equal volumes of hot liquid and cool is highly improbable.

Another mechanism has been recently proposed by Moore and Mesler (15). They measured temperature drops on the heat transfer surface in a boiling water system with a special thermocouple designed to measure the temperature of a small area and to have a microsecond response time. The temperature, as observed on an oscilloscope, dropped occasionally 20-30° F in about two milliseconds. Moore and Mesler calculated the heat removed per temperature drop by theoretical considerations. Multiplication of these values by the frequency of drops gave values which were 70-90% of the average heat flux. From this information they proposed the theory that the large heat fluxes in boiling came from vaporization of a micro-layer, 78-89 microinches thick in this investigation, of liquid at the base of the bubble.

Of the four mechanisms discussed, the vapor – liquid exchange and the vaporization of a micro-layer of liquid at the base of the bubbles appear to be the best theories to explain the high heat fluxes obtained when liquids are boiled.

These mechanisms do not explain how the bubbles themselves form. As its name implies, nucleate boiling is a nucleation process. Sources of nuclei which have been postulated include: cavities and scratches on the

boiling surface, points of low adhesion along the liquid metal interface, solid particles suspended in the liquid, ions formed by radiation or strong electric fields, microscopic spines on the solid, grain boundaries on the surface, specks of dirt or oxide adhering to the solid. Bankoff (1,2) concluded from theoretical considerations that bubbles probably form from preexisting microscopic vapor or gas bubbles trapped in cavities or grooves on the solid surface. Microphotographs taken by Clark, Strenge, and Westwater (4) confirm Bankoff's theory.

Corty and Foust (5) investigated the effect of surface roughness on boiling heat transfer rates from nickel to n - pentane. For different polishes, the boiling curves changed. The rougher the polish, the higher the heat flux was for a given temperature excess. The roughness as measured by a profilometer ranged from 2 to 25 root mean square micro-inches. Jakob also showed this same characteristic with water as his boiling liquid (13). Both investigations also showed slight changes in the slopes of the boiling curves.

In order to study nucleation, we have to make assumptions as to the nature of the surface roughness. Two types of cavities which are amenable to mathematical analysis are shown in Fig. 3. The radius of curvature of the interface between the liquid and vapor can be approximated by the Thompson relation:

$$(2) \qquad \Delta P = \frac{2s}{r}$$

where ΔP is the pressure difference between the inside and outside of the bubble and s is the surface tension. When the bubble is at equilibrium, the vapor must be at the saturation temperature corresponding to the inter-

nal pressure, and the liquid also must be at this temperature. Consequent-
ly, the liquid is superheated, and its temperature excess can be related
to the pressure excess, ΔP, by the Clapeyron equation. For small ranges
the derivative can be approximated by $\frac{\Delta P}{\Delta T}$ and the resulting relation yields:

(3) $\quad \frac{\Delta P}{\Delta T} = \frac{P_i - P_\infty}{T_w - T_s} = \frac{\lambda}{T(V_v - V_L)}$ $\quad$ (See Nomenclature for meaning of symbols)

Thus, we can express r in terms of T_x:

(4) $\quad r \quad \dfrac{2s \; T \; (V_v - V_L)}{\lambda \; T_x}$

The appropriate value for T would be a mean value between T_w and T_s, but
little error would result by using either T_w or T_s. At low pressures V_v
would be large compared to V_1 so V_1 could be dropped. The radius of the
initial bubble can be related to the dimensions of the idealized conical
cavity in Fig. 3a by the following:

(5) $\quad r_i = \dfrac{d_i}{\cos \; (\theta - \emptyset/2)}$, $\quad i = 0,1$

Griffith and Wallis have made plots of reciprocal radius versus bubble
volume for the two types of conical cavities, assuming a contact angle θ, of
$90°$ (9). These are reproduced beneath the appropriate cavities in Fig. 3.
The radius of curvature passes through a minimum to produce a bubble at the
site. This occurs when the bubble radius equals one-half the diameter of
the cavity at the surface. This will remain the same provided $\emptyset/2 < \theta < 90$.
If θ is less than $\emptyset/2$, no minimum will occur. If θ is greater than $90°$,
the temperature excess required to initiate boiling will be reduced.

Experiments have been conducted to determine if Equation (4) actually describes the situation (9). A surface on which there was a cavity of known geometry was immersed in a liquid. The pressure and temperature of the liquid were adjusted until boiling from the cavity nearly ceased. The values at this point were used to calculate the superheat, T_x. The experimental results were very close to values calculated from the equation.

An attempt was then made to predict results of boiling from a surface with several identical cavities of known dimensions. With several identical cavities, one would expect a portion of the boiling curve to be vertical. Although the resulting curve was steep, the line was not vertical. Also, the wall superheats were considerably larger than expected ($20^\circ F$ as opposed to $3^\circ F$). Possible explanation for these results include: the cavities are not the nucleate sites, the mean surface temperature is not that seen by the cavities, the nucleation properties of a cavity are not determined by the equation. The conclusion reached by Griffith and Wallis is that the temperature felt by an active cavity was not the mean surface temperature.

Many investigators have proposed correlations relating the variables in nucleate boiling (21,22). Some have included parameters to describe the surface; some have not. Many of the correlations consist of relating groups of dimensionless numbers. Some of the authors have based their correlations on models and theories, while others have used just "brute-force" correlation of variables. Westwater has collected many correlations published since 1952 (22).

IV. DISCUSSION

Although there has been considerable work done on the problem of predicting boiling heat transfer rates, researchers have been plagued by poor reproducibility of results. Probably the chief reason for this scatter of data has been the varied conditions of the heat transfer surfaces. The purpose of this research project was to eliminate this effect on the heat flux, and to study the effects of liquid properties on the boiling heat transfer rates.

The first approach was to use lengths of copper wire from the same spool prepared in the same manner before boiling. This way the nature and magnitude of the surface roughness were expected to be the same for each boiling experiment. Oxidation would affect the surface roughness, so the potential leads were not silver-soldered to the boiling wire. Instead, small slits were made on the wire approximately 2.5 inches apart. The potential leads were inserted, and the burrs raised from making the slits were clamped down upon the leads. Only a negligible portion of the wire between these leads was disturbed by this procedure.

The copper wires were degreased with an acetone wash, etched with a one-minute wash in a 25 volume per cent aqueous solution of nitric acid, washed with tap water, and rinsed in carbon tetrachloride before being inserted into the boiler. As the power was increased in increments, the heat flux followed the natural convection curve (see Fig. 8) until boiling started.

Until the nucleate sites were evenly distributed along the wire, the data points fell somewhere between the convection curve and the "normal" boiling curve. This is an example of the hysteresis observed by previous

investigators. Hysteresis is probably caused by the uneven distribution of nucleate sites which develops during increasing flux. A portion of the heat is transferred by convection; another, by boiling. In a well-degassed system data points jump immediately from high superheats on the natural convection curve to the "normal" boiling heat flux curve at considerably lower superheats (16). In such systems boiling spreads quickly and uniformly over the entire heat transfer surface.

A glance at the boiling curves for the copper-carbon tetrachloride system (see Fig. 8) reveals a different type of hysteresis. The path of decreasing flux is at slightly higher superheats than the corresponding path of increasing flux. This aging effect has been noted before (16). In this case it is likely that the roughness and chemical nature of the surface was changed by the formation of copper chloride on the wire, as a definite tarnishing occurred during the boiling run. Curves 1, 2, 3, and 4 came from the same wire, but the wire was given a 3-minute acid wash before the data for curve 4 were taken. The shifting of the curve to the left appears to confirm the theory that the aging effect was due to the formation of a different type of surface which could be at least partially reverted towards the original form by a chemical treatment. Whether this tarnished surface changed the heat flux curves because the roughness changed or the chemical nature changed was not established.

Curves 5 and 6 of Fig. 8 come from the data obtained from two new lengths of copper wire which had potential leads silver-soldered to them. The scale from oxidation of the copper near the connection was removed by the acid wash, but the surface was left roughened by the treatment. Note

the odd point near curve 1 which should be on curve 5. This was the first

point of nucleate boiling. At this time the run had to be delayed while

the heater in the insulating box was repaired. Apparently the delay was

enough to cause the wire to age before the remainder of the data was taken.

The close proximity of curve 6, the increasing flux portion of curve

1, and the aforementioned odd point of curve 5 indicate the idea behind

this attempt to eliminate the effect of the surface on boiling heat flux

was good. However, the aging effect proved to be a major problem. To

nullify this effect, all further runs used a chemically inert surface, a

20-gauge gold wire.

The natural convection curves are shown in Figures 4-7. Comparison

of natural convection curves for the gold and copper wires indicates sur-

face has no effect on this method of heat transfer. This is expected, as

no correlations for natural convection include any terms taking the kind

or nature of surface into account. Two characteristics of these curves

are quite evident--the scatter of data about each curve is very minimal,

and the curves for all liquids are similar, nearly coincident in some cases.

The nucleate pool boiling data using the gold wire as the heat trans-

fer surface are given in Table 1. The heat flux versus temperature excess

curves for the eight liquids with the gold heat transfer surface are pre-

sented in Figures 9-16. Included on these figures are the nucleate site

population versus temperature excess curves which correspond to the heat

flux curves. Good reproducibility, particularly for the heat flux curves,

is evident for carbon tetrachloride, chloroform, trichloroethane, and

cyclohexane. A drift similar to that caused by aging appears in the

benzene and ethylene dichloride curves. The curves for ethyl acetate and trichloroethylene are extreme examples of drift. The phenomenon of increasing temperature excess with decreasing heat flux in the nucleate boiling region has never been reported previously. The cause of this queer behavior was not evident until the boiler was disassembled following the runs with trichloroethylene. Spots of a light ash-like material covered the gold wire. This led to the hypothesis that these liquids were such excellent solvents that the Epon resin and possibly the stopcock grease were dissolved in the condensing vapors, returned to the liquid pool, and deposited on the wire when the liquid at the hot surface evaporated into vapor bubbles.

The difference in the boiling curves for the different liquids studied in this investigation can be restricted to two features--the temperature excess at which the nucleate boiling region starts, and the magnitude of the slope of the curve in the nucleate region. If the temperature excess at which boiling begins is related to the size of cavities on the boiling surface, the relationship of Equation (4) should be a reasonable starting point for the analysis of this feature. A plot of nucleate population versus the r calculated from this equation is presented in Figure 17. In order to simplify the calculations, the physical properties of the liquids at their boiling points (T_s) were used. In addition T_w was used in place of T_{mean}. These simplifications appear to be reasonable since the T_x's only ranged 10-30°F. The error in measurement of the liquid properties, particularly at temperatures near the boiling point, probably contribute more to the variation of r than these simplications. Since the data points

for the boiling curves of the second and following runs with ethyl acetate, ethylene dichloride, and trichloroethylene, were shifted considerably, only the data from the first runs for these liquids were used for Figure 17.

Each liquid exhibits the expected characteristics of more nucleate sites at lower values of r. This figure could be thought of as a portion of a distribution curve. Bubble columns start appearing at the sites larger in diameter first. Then the smaller sites start contributing bubble columns as the temperature of the surface increases. The distribution of cavity sizes could only be determined over the range in which it was possible to obtain visual counts of the active nucleate sites. From Figure 17 we can conclude that the majority of sites active at the temperatures studied correspond to cavities with equivalent radii of 2-4 x 10^{-6} ft.

If the size distribution, or equivalent size distribution, of potential sites on a surface could be determined, it appears theoretically possible to predict the number of sites which would be active at a given temperature excess through use of Equation (4). This size distribution could possibly be determined by boiling one liquid whose physical properties are well known and plotting the results on a figure similar to Figure 17. We could then assume this curve also held for other liquids. Thus we could calculate N versus T_x curves for any liquid whose physical properties are known. This method likens boiling heat transfer work to kinetics; laboratory work must be done before design work.

If we are at the point where we have an N versus T_x curve, we would still need to know how heat flux is dependent on N. Jakob (13) reported that the heat flux in boiling water was directly proportional to N. Later

work (20) has indicated the relationship should be

(6) $\qquad \frac{Q}{A} \propto \sqrt{N} = N^{\frac{1}{2}}$

Nickelson (16) substantiated Jakob's relation,

(7) $\qquad \frac{Q}{A} \propto N$

with a system of carbon tetrachloride on fresh gold, silver, and copper

surfaces. However, his k's were different for each type of surface and

each pressure he studied. He also corrected his heat flux data by sub-

tracting the contribution due to natural convection at the given T_x he was

considering.

Figure 18 is a log-log plot of heat flux versus N for the runs with

the gold wire in this investigation. On such a plot the slope of the curve

would give the exponent in the relation

(8) $\qquad \frac{Q}{A} = k \, N^a$

No corrections for natural convection were taken. Notice that the curves

are different for each liquid. For reference, straight lines with slopes

of one-half and one are included on the figure. It is readily discernible

that the slopes lie in this range, but it is not possible to state defi-

nitely that the heat flux for all liquids is proportional to either N or

$\sqrt{N}$. Whereas the curve for chloroform appears to have a slope nearly equal

to one, the curves for trichloroethane, ethyl acetate, and trichloroethylene

have slopes closer to one-half. Some of the curves do not have constant

slopes over the range studied. Instead, the slopes increase as the site

population increases, but they still remain in the range of one-half to one.

In order to examine this relation between heat flux and nucleate site

population in greater detail, the heat contribution per nucleate site was determined for all data points where the number of sites was greater than 10 ($N = 38.9$). Below this value accurate site counts were impossible to get because the sites would die out, re-activate, and die out again. This cycling was too erratic to obtain even a good average value for the number of sites which were active.

At low T_x's the contribution of natural convection to the total heat flux is significant. Therefore, the value of the heat flux on the convection curve corresponding to the T_x of the point being studied was subtracted from the overall heat flux at this T_x. The resulting difference, Q_n/A, was then divided by the nucleate population, $N = n/A$, to get the heat contribution per nucleate boiling site, Q_n/n. If the heat flux contribution due to the nucleate boiling was directly proportional to the number of sites, the values for Q_n/n would be constant for any one liquid. Figures 19-22 indicate this conclusion cannot be drawn for all liquids. These plots of Q_n/n versus N reveal that the data points for some liquids, notably trichloroethane, carbon tetrachloride, and ethyl acetate, tend to group themselves about a horizontal line, but the points for the other liquids begin to rise with increasing N, particular beyond $N = 200$. This "curling" upward might be due to low counts of N at these higher heat fluxes. Many of the individual sites could have been missed during the counting because they were obscured by other bubble columns or their bubbles coalesced with those from other sites. This does not explain the very definite continuously upward trend of the data points for chloroform.

From the data presented in Figures 18-22, we can conclude that neither

the total heat flux nor the nucleate boiling contribution to the total
flux is always directly proportional to the population of nucleate boiling
sites. Nor is either of these values always proportional to the square
root of the site population. The heat flux for each boiling liquid has its
own functional relationship to the active boiling sites. From the data
in this investigation, the following general conclusions about Q_n/n can
be drawn: the steeper the heat flux versus T_x curve is during the nucle-
ate boiling region, the more closely Q_n/n versus N approaches a horizontal
line; the greater the T_x is at which nucleation begins, the higher the
values for Q_n/n will be. Evidently Q_n/n, as well as Q/A, is highly de-
pendent on T_x.

If we can use the heat transfer mechanism proposed by Forster and
Grief (7), the ratio M of Equation (1) should be an indicator of the change
in magnitude due to the change in T_x. Assuming the temperature of the
liquid is nearly T_s and the temperature gradient in the liquid is linear
over the radial distance from the heat source, the ΔT_{mean} would range
roughly from 7-15 in this study. If we compare trichloroethylene to
trichloroethane, we can see Q_n/n for trichloroethylene is about twice as
great as that for trichloroethane. The ratio of M's is approximately

$$\frac{M_2}{M_1} = \frac{C_{L2} \, \rho_{L2} \, \rho_{v1} \, \lambda_1 \, \Delta T_{mean\,2}}{C_{L1} \, \rho_{L1} \, \rho_{v2} \, \lambda_2 \, \Delta T_{mean\,1}}$$

$$\frac{(0.34) \, (82) \, (0.31) \, (104) \, (17)}{(0.27) \, (78) \, (0.29) \, (103) \, (14)} = 1.7$$

Of course, we do not know the ratio of latent heat transport with trichloro-
ethylene to that with trichloroethane, since we have no information on

bubble size or frequency. If the latent heat transport ratio were unity or slightly more, this ratio of M's could explain the difference in Q_n/n's for these two liquids.

V. MULTIPLE REGRESSION

The object of investigating physical or chemical phenomena is to obtain information which can ultimately be put to practical use. If a mathematical model can be found to describe the physical situation, the relationship among the variables can be examined in detail and results obtainable from conditions yet untested can be predicted.

Until recently, the tool used most extensively for correlation of variables in chemical engineering research has been dimensional analysis. This method consists of assuming a model of the form

$$(9) \qquad N_1 = c_0 \, (N_2)^a \, (N_3)^b \, (N_4)^c \, \ldots$$

where N_1, N_2, etc. are dimensionless numbers such as Reynolds number, Prandtl number and Nusselt number. The constants c_0, a, b, c, ... are usually determined from appropriate cross plots on logarithmic graph paper.

Lately, statistical methods have been applied to chemical engineering problems. The method of multiple linear regression is particularly suited to studying functional relations among variables. In general we consider a mathematical model of the following type:

$$(10) \qquad Y_i = B_0 + B_1 X_{1_i} + B_2 X_{2_i} + \ldots + B_k X_{k_i} + \epsilon_i$$

where $i = 1, 2, \ldots, n$ and ϵ_i are random variables which are normally and independently distributed about a mean of zero with a variance of σ^2 ($\epsilon_i \sim NID \, (o, \sigma^2)$). In matrix notation the above relationship is written as

(11) $\quad Y = XB + \epsilon$

where

$$Y = \begin{pmatrix} Y_1 \\ Y_2 \\ \cdot \\ \cdot \\ \cdot \\ Y_n \end{pmatrix}$$

$$X = \begin{pmatrix} 1 & X_{11} & X_{21} & \cdots & X_{k1} \\ 1 & X_{12} & X_{22} & \cdots & X_{k2} \\ \cdot \\ \cdot \\ \cdot \\ 1 & X_{1k} & \cdots & X_{kn} \end{pmatrix}$$

$$B = \begin{pmatrix} B_0 \\ B_1 \\ \cdot \\ \cdot \\ \cdot \\ B_k \end{pmatrix}$$

$$\epsilon = \begin{pmatrix} \epsilon_1 \\ \epsilon_2 \\ \cdot \\ \cdot \\ \epsilon_n \end{pmatrix}$$

The problem is to find estimators for the unknown parameters B_1, B_2, $\ldots$, B_k. The matrix of estimators is

$$\hat{B} = \begin{pmatrix} b_o \\ b_1 \\ \circ \\ \bullet \\ \circ \\ b_k \end{pmatrix}$$

This problem can be handled through the principle of maximum likelihood. If the probability function of a random vector $\underline{X}$ is $f(X_i ; \Theta_1, \Theta_2, \ldots, \Theta_k)$ where the Θ's are some unknown parameters and the X_i's are independent, then the likelihood function is

$$(12) \quad L = \prod_{i=1}^{n} f(X_i ; \Theta_1, \Theta_2, \ldots, \Theta_k)$$

The maximum likelihood estimators of $\Theta_1, \ldots, \Theta_k$ are those numbers which maximize L for a given set X_1, X_2, $\ldots$, X_n.

The likelihood function for the multiple regression model is

$$(13) \quad L = \left(\frac{1}{2\pi\sigma^2}\right)^{\frac{n}{2}} \exp\left[-\frac{1}{2\sigma^2} \sum_{i=1}^{n} (Y_i - B_o - B_1 X_{1i} - \ldots \ldots - B_k X_{ki})^2 \right]$$

or in matrix notation

$$(14) \quad L = \left(\frac{1}{2\pi\sigma^2}\right)^{\frac{n}{2}} \exp\left[-\frac{1}{2\sigma^2} \epsilon' \epsilon \right]$$

$$(15) \quad = \left(\frac{1}{2\pi\sigma^2}\right)^{\frac{n}{2}} \exp\left[-\frac{1}{2\sigma^2} (Y - XB)' (Y - XB) \right]$$

where the primes indicate the transpose of the matrix. The values of the parameters which maximize L are found in the classical manner—by taking the partial derivatives of L with respect to the unknown parameters, equating them to zero, and solving the resulting equations. In this case it is easier to differentiate the function

$$(16) \quad \ln L = c - \frac{n}{2} \ln \sigma^2 - \frac{1}{2\sigma^2} \sum_{i=1}^{n} (Y_i - B_0 - B_1 X_{1_i} - \ldots B_k X_{k_i})^2$$

Let b_j $(j = 0, 1, 2, \ldots, k)$ be the maximum likelihood estimators of B_0, $B_1, \ldots, B_k$; and $\hat{\sigma}^2$, that of σ^2. The equations resulting from equating the partial derivatives to zero are

$$(17) \quad \hat{\sigma}^2 = \frac{1}{n} \sum_{i=1}^{n} (Y_i - b_0 - b_{1_i} X_1 - \ldots - b_k X_{k_i})^2$$

$$(18) \quad nb_0 + b_1 \sum_{i=1}^{n} X_{1_i} + \ldots + b_k \sum_{i=1}^{n} X_{k_i} = \sum_{i=1}^{n} Y_i$$

$$(19) \quad \sum_{i=1}^{n} X_{1_i} b_0 + b_1 \sum_{i=1}^{n} X_{1_i}^2 + \ldots + b_k \sum_{i=1}^{n} X_{k_i} = \sum_{i=1}^{n} Y_i X_{1_i}$$

$$(20) \quad \sum_{i=1}^{n} X_{k_i} b_0 + \ldots + b_k \sum_{i=1}^{n} X_{k_i}^2 = \sum_{i=1}^{n} Y_i X_{k_i}$$

In matrix rotation the equations of estimation for B are

$$(21) \quad X' X \hat{B} = X' Y$$

Let $S = X'X$. If S is non-singular (has an inverse), then

$$(22) \quad \hat{B} = S^{-1} X' Y$$

In this investigation the mathematical model assumed was

$$(23) \quad \left(\frac{Q}{A}\right)_i = 10^{B_0 + \epsilon_i} \, T_{x_i}^{B_1} \, t_{w_i}^{B_2} \, \Lambda_i^{B_3} \, \rho_{L_i}^{B_4} \, \rho_{V_i}^{B_5} \, s_i^{B_6} \, c_{L_i}^{B_7} \, \mu_{L_i}^{B_8} \, k_{L_i}^{B_9}$$

where $i = 1, 2, \ldots, 225$

The method of linear regression was applied to the model

$$(24) \quad \left(\log \frac{Q}{A}\right)_i = B_0 + B_1 \left(\log T_x\right)_i + B_2 \left(\log t_w\right)_i + \ldots + B_9 \left(\log k_L\right)_i + \epsilon_i$$

In this equation $\log \frac{Q}{A}$ corresponds to Y of equation (10), $\log T_x$ to X_1, etc.

Many of the physical properties of these liquids had to be determined by extrapolation and estimation. Because of the inherent error from these calculations, it was felt very little additional error would result from using the values of these properties at the boiling point rather than at a mean temperature between the saturation temperature (boiling point) and the heating surface temperature. The values used for the regression analysis are listed in Table II. In order to obtain a realistic correlation, the data from the ethyl acetate runs were not included. Also, only the initial runs with ethylene dichloride and trichloroethylene were used in the analysis. These were the runs which had extreme drift due to deposits on the surface. In this way it is reasonably certain that the regression applies only to a constant surface. There may be some question as to the advisability of using the data from the second and third benzene

runs, but they were included because the drift towards higher temperature

excesses was not as noticeable as that for the previously noted liquids.

Only data taken during nucleate boiling were included in this regression

analysis. All calculations, including the transformation of Equation 23

to Equation 24, were done on an IBM 1620 data processing machine.

The estimates of the B's found from the regression analysis, together

with their variances, are as follows:

exponent of 10, b_0 = 10.382

" T_x, b_1 = 3.224 $V(b_1)$ = 0.0162

" t_w, b_2 = -2.463 $V(b_2)$ = 0.4694

" λ, b_3 = -2.676 $V(b_3)$ = 4.1910

" ρ_L, b_4 = 1.831 $V(b_4)$ = 0.2505

" ρ_v, b_5 = -3.087 $V(b_5)$ = 7.1196

" s, b_6 = 0.846 $V(b_6)$ = 0.9201

" C_L, b_7 = 4.057 $V(b_7)$ = 0.4814

" μ_L, b_8 = 6.859 $V(b_8)$ = 0.2362

" k_L, b_9 = 0.388 $V(b_9)$ = 0.0403

The unbiased estimate of the variance is 0.008314. The coefficient of

multiple correlation, R^2, is 0.861. Since a perfect correlation would

give an R^2 equal to one, this correlation is quite good.

An idea of the importance of each variable in the correlation can

be obtained by examining the loss in sums of squares by deleting each

variable. The greater this value, the more important the variable is in

the correlation. The variables are listed below in decreasing importance

by this criterion:

Variable	Loss in Sums of Squares	F Test
T_x	5.332	641.3
μ_L	1.656	199.2
c_L	0.2843	34.19
ρ_L	0.1113	13.38
t_w	0.1075	12.92
k_L	0.03103	3.733
λ	0.01421	1.709
ρ_v	0.01113	1.338
s	0.006465	0.7775

The critical F for testing the hypothesis that $B_i = 0$ with a Type I error of 5% is 3.89. Thus, we must conclude that any one of the exponents on k_L, λ, ρ_v, or s is not significantly different from zero when tested alone. In order to go any further, the analysis would have to be corrected for the deletion of the one chosen variable. This can be done by methods described in books on statistical methods (6, 18).

In the comparison of this correlation to others which have been proposed, the confidence limits on the b_i's are of importance. These are calculated from the relations

$$L_1 = b_i - t_{\alpha(n-k-1)} \hat{\sigma}_{b_i}$$

$$L_2 = b_i + t_{\alpha(n-k-1)} \hat{\sigma}_{b_i}$$

where α is the probability of Type I error, n-k-1 represents the degrees

of freedom, and $\hat{\sigma}_{b_i}$ is the estimate of the standard deviation of b_i (the

positive square root of the estimated variance of b_i). The 95% confidence

limits for the b_i's found in this investigation are as follows:

$$2.973 < \text{exponent of } T_x < 3.475$$
$$5.901 < \text{exponent of } \mu_L < 7.817$$
$$2.690 < \text{exponent of } C_L < 5.424$$
$$0.844 < \text{exponent of } \rho_L < 2.818$$
$$-3.813 < \text{exponent of } T_w < -1.113$$
$$-0.008 < \text{exponent of } k_L < 0.784$$
$$-6.716 < \text{exponent of } \lambda < 1.364$$
$$-8.347 < \text{exponent of } \rho_v < 2.173$$
$$-1.044 < \text{exponent of } s < 2.736$$

The b_i's and their confidence limits permit us to compare this correla-

tion with those presented by others. Table III presents a summary of

exponents from other correlations as presented in Westwater's article (22)

together with the results of this study.

This correlation for nucleate boiling should not be used indiscrimi-

nately. Because surface roughness and nature have major effects on the

heat transfer, this correlation would be used best to predict the change

in heat transfer by a change in T_x and t_w or by a change in liquids by

computing the ratio

$$\frac{Q/A \text{ proposed}}{Q/A \text{ known}}$$

from the terms in the correlation. This means, heat transfer data for some

liquid in the system under study should be known before predicting heat

fluxes from this correlation.

VI. SUMMARY

This investigation of boiling heat transfer studied the effect of the properties of several liquids on the heat flux, keeping a constant surface. The results showed that the heat flux was not always proportional to the nucleate site population nor to the square root of the population, but fell somewhere within these limits depending on the liquid being boiled. The nucleate heat transfer rate (Q_n) per bubble site varied with the liquid studied. Those liquids which had steep boiling curves tended to have a constant heat transfer rate per site. The liquids with boiling curves of smaller slope had higher heat transfer rates per site as the number of sites increased. Higher rates per site occurred with liquids which started nucleate boiling at higher temperature excesses. This indicates that the heat transfer rate per nucleate site was highly dependent on the temperature of the heat transfer surface.

The theory of multiple linear regression was applied to develop a correlation for the heat flux during nucleate pool boiling. The resulting equation was:

$$\frac{Q}{A} = 2.41 \times 10^{10} \; T_x^{3.244} \; t_w^{-2.463} \; \lambda^{-2.676} \; \rho_L^{1.831} \; \rho_v^{-3.087}$$

$$s^{0.846} \; C_L^{4.057} \; \mu_L^{6.859} \; k_L^{0.388}$$

The variables listed in order of decreasing importance by the criterion of loss in sums of squares by deletion of the variable were:

$$T_x, \; \mu_L, \; C_L, \; \rho_L, \; t_w, \; k_L, \; \lambda, \; \rho_v, \; s$$

APPENDIX

NOMENCLATURE

a   A Numerical constant

A   Area perpendicular to flow of heat

B_i Coefficient in regression model

Btu   British thermal unit

C_L Heat capacity of liquid, Btu/lb- F

D   Characteristic length in some boiling heat transfer correlations

$°F$ Degrees Fahrenheit

ft   Feet

g   Acceleration, ft/hr^2

hr   Hour

k   Proportionality constant

k_L Thermal conductivity of liquid, Btu/hr-ft- F

KVA   Kilovolt - amperes

lb   Pounds

ln   Logarithm to base e

log   Logarithm to base 10

mm   Millimeters

M   Ratio of heat transferred by liquid-vapor exchange to that transferred by latent heat

n   Number of nucleate boiling sites

N   Nucleate site population, n/A, in^{-2}

N_i Dimensionless number

P   Pressure, lb/ft^2

P_c	Critical pressure, lb/ft^2
P_i	Internal pressure of bubble, lb/ft^2
P_x	Pressure difference corresponding to T_x, lb/ft^2
P_∞	Vapor pressure corresponding to T_s, lb/ft^2
Q/A	Heat flux, $Btu/hr\text{-}ft^2$
Q_n	Total heat transfer rate minus heat transfer rate due to natural convection
r	Radius of bubble
r^*	Radius of ideal conical site, ft
s	Surface tension, lb/ft
sec	Seconds
sq	Square
T	Temperature, R
T_s	Temperature of saturation
t_w	Temperature of heat transfer surface, F
T_w	Temperature of heat transfer surface, R
T_x	Temperature excess, $T_w\text{-}T_s$
V_B	Bubble volume, ft^3
V_L	Volume of liquid, ft^3
V_v	Volume of vapor, ft^3
X_i	Independent variable in regression model
Y_i	Dependent variable in regression model
λ	Latent heat of vaporization, Btu/lb
ρ_L	Density of liquid, lb/ft^3

ρ_v Density of vapor, lb/ft^3

$\propto$ "Is proportional to"

ϵ_i Random variable in regression model

θ Contact angle liquid makes with heating surface

θ_i Parameter in probability distribution

ϕ Apex angle of conical cavity

σ^2 Variance

μ_L Viscosity of liquid, $lb/ft\text{-}hr$

TABLE I. NUCLEATE POOL BOILING DATA WITH GOLD WIRE AS HEAT TRANSFER SURFACE

T_w, $^\circ F$	T_x, $^\circ F$	Q/A, Btu/hr-ft^2	N, Sites/in^2	Q_n/n Btu/hr-site
		Carbon Tetrachloride – Run 1		
195.6	25.6	11,820	–	
195.2	25.2	10,520	–	
194.8	24.8	9,730	–	
195.0	25.0	10,180	–	
194.4	24.4	8,460	249	0.158
193.9	23.9	7,760	233	.150
193.4	23.4	6,660	222	.126
192.8	22.9	5,790	175	.128
191.4	21.4	4,800	140	.121
190.7	20.7	3,940	109	.106
189.8	19.8	3,450	77.9	.116
189.4	19.4	3,110	81.6	.085
189.7	19.7	3,490	89.5	.105
188.0	18.0	2,610	54.5	.089
186.4	16.4	2,110	31.1	.094
184.2	14.2	1,640	19.4	.429
		Carbon Tetrachloride – Run 2		
195.1	24.1	9,210	–	
194.8	23.8	8,300	272	.143
194.4	23.4	7,560	253	.135
193.8	22.8	6,690	206	.138
193.3	22.3	5,730	182.8	.123
192.9	21.9	5,190	143.9	.133
192.5	21.5	4,730	136.2	.119
191.9	20.9	4,320	112.8	.124
191.6	20.6	3,920	101.2	.114
191.3	20.3	3,590	73.9	.129
191.1	20.1	3,380	66.1	.126
190.0	19.0	2,660	27.2	.158
189.0	18.0	2,290	23.3	.081
		Carbon Tetrachloride – Run 3		
193.1	23.2	7,190	214	.149
192.2	22.3	5,980	–	
193.5	23.6	7,950	245	.150
192.8	22.9	6,510	175	.156
192.0	22.1	5,710	163.3	.138
191.5	21.6	5,040	132.2	.139

TABLE I (Continued)

T_w, ^{o}F	T_x, ^{o}F	Q/A, Btu/hr-ft^2	N, Sites/in^2	Q_n/n Btu/hr-site
		Carbon Tetrachloride - Run 3 (Continued)		
191.1	21.2	4,650	120.7	0.133
190.7	20.8	4,310	105	.134
190.4	20.5	3,730	66.1	.158
189.6	19.7	3,260	58.4	.133
188.5	18.6	2,750	31.1	.172
		Carbon Tetrachloride - Run 4		
196.6	26.6	14,120	--	
195.5	25.5	11,880	--	
194.8	24.8	10,480	327	.163
193.9	23.9	9,090	288	.154
192.8	22.8	7,780	241	.151
192.1	22.1	6,660	237	.123
191.5	21.5	5,910	202	.121
191.0	21.0	5,130	179.0	.109
189.9	19.9	4,140	140.2	.098
188.5	18.5	3,330	101.2	.093
186.8	16.8	2,720	66.1	.103
183.7	13.7	1,638	23.4	.089
		Chloroform - Run 1		
168.2	26.1	8,740	249	.162
168.8	26.7	8,330	233.5	.158
168.6	26.5	7,570	190.8	.167
168.2	26.1	7,030	182.9	.156
167.3	25.2	6,040	155.7	.145
166.1	24.0	5,340	132.3	.142
165.8	23.7	4,960	128.4	.128
164.1	22.0	4,390	109.0	.128
162.7	20.6	3,920	105.1	.114
160.9	18.8	3,400	93.4	.109
157.8	15.7	2,230	66.1	.072
156.4	14.3	1,928	46.7	.081
		Chloroform - Run 2		
172.8	30.5	12,270	--	
173.4	31.1	13,170	--	
174.1	31.8	14,010	--	
174.5	32.2	14,900	--	

TABLE I (Continued)

T_w, °F	T_x, °F	Q/A, Btu/hr-ft^2	N, Sites/in^2	Q_n/n Btu/hr-site

Chloroform - Run 2 (Continued)

175.7	33.4	17,320	–	
172.8	30.5	11,730	315	0.181
172.4	30.1	10,880	284	.182
171.0	28.7	9,490	264.5	.163
170.8	28.5	8,790	233.5	.165
170.4	28.1	8,100	229.5	.148
169.4	27.1	7,390	237.5	.126
168.2	25.9	6,530	210.0	.120
167.2	24.9	5,950	186.8	.119
165.7	23.4	5,100	163.4	.107
165.0	22.7	4,640	151.8	.099
164.4	22.1	4,500	144.0	.102
163.3	21.0	4,160	124.6	.107
163.0	20.7	3,880	120.7	.096
162.0	19.7	3,600	109.0	.098
161.3	19.0	3,330	97.4	.097
160.6	18.3	2,930	93.4	.078
159.5	17.2	2,680	77.9	.084
158.5	16.2	2,360	66.1	.078
157.3	15.0	2,090	58.4	.073
156.2	13.9	1,782	54.5	.056
154.0	11.7	1,410	38.9	.059
152.3	10.0	1,034	23.4	.046

1,1,1 - Trichloroethane - Run 1

193.9	28.5	13,130	–	
193.9	28.5	11,920	–	
193.8	28.4	10,500	–	
193.7	28.3	9,500	–	
193.6	28.2	8,870	350	.118
193.5	28.1	8,000	304	.116
193.3	27.9	7,320	280	.110
193.0	27.6	6,670	245	.108
192.2	26.8	5,560	190.7	.102
192.2	26.8	5,250	182.9	.095
191.5	26.1	4,380	108.9	.110
190.7	25.3	4,010	85.6	.118
190.2	24.8	3,500	66.1	.107
188.6	23.2	3,110	38.9	.150

TABLE I (Continued)

T_w, $^{\circ}F$	T_x, $^{\circ}F$	Q/A, Btu/hr-ft^2	N, Sites/in^2	Q_n/n Btu/hr-site
		Trichloroethane – Run 2		
194.0	28.6	9,550	–	
193.8	28.4	8,660	366	0.108
193.5	28.1	7,350	296	.104
193.3	27.9	6,300	241	.098
192.9	27.5	5,860	202	.103
192.8	27.4	5,450	194.7	.093
192.6	27.2	5,130	182.9	.088
192.0	26.6	4,590	124.6	.104
191.8	26.4	4,320	97.3	.116
191.1	25.7	3,900	77.9	.119
190.7	25.3	3,680	77.9	.102
190.2	24.8	3,370	62.3	.099
190.0	24.6	2,860	42.8	.066
188.5	23.1	2,440	27.2	.048
187.3	21.9	2,140	15.6	.022
		Benzene – Run 1		
203.6	27.4	12,210	300	.185
203.4	27.2	11,780	253	.208
203.2	27.0	11,090	234	.206
203.1	26.9	10,230	226	.186
203.0	26.8	9,310	202	.177
202.8	26.6	8,860	202	.162
202.7	26.5	8,310	175.2	.168
202.7	26.5	7,980	163.4	.166
202.5	26.3	7,460	147.8	.160
202.3	26.1	6,950	112.8	.180
202.1	25.9	6,560	112.8	.159
202.0	25.8	6,240	105.1	.151
201.9	25.7	5,910	93.4	.147
201.6	25.4	5,540	70.1	.164
201.2	25.0	5,120	70.1	.129
		Benzene – Run 2		
204.4	28.2	13,820	–	
204.1	27.9	12,100	257	.210
204.0	27.8	11,130	245	.193
203.9	27.7	10,620	241	.182
203.8	27.6	9,760	202	.188
203.7	27.5	8,890	182.8	.176

TABLE I (Continued)

T_w, °F	T_x, °F	Q/A, Btu/hr-ft²	N, Sites/in²	Q_n/n Btu/hr-site
		Benzene - Run 2 (Continued)		
203.6	27.4	8,270	167.3	0.167
203.6	27.4	7,800	155.7	.159
203.2	27.0	7,040	144.0	.133
203.1	26.9	6,500	105.1	.155
202.8	26.6	5,930	77.9	.166
202.5	26.3	5,420	66.2	.144
202.1	25.9	4,960	46.7	.147
201.2	25.0	4,270	38.1	.082
		Benzene - Run 3		
204.6	28.4	12,780	284	.204
204.3	28.1	11,080	253	.184
204.4	28.2	10,630	226	.192
204.3	28.1	9,610	186.8	.195
204.1	27.9	8,710	171.2	.178
204.0	27.8	8,290	159.6	.171
203.9	27.7	7,760	136.2	.177
203.7	27.5	7,020	124.6	.154
203.8	27.6	6,710	97.3	.174
203.5	27.3	6,390	81.7	.184
203.0	26.8	5,850	62.3	.186
202.5	26.3	5,110	42.8	.174
		Ethyl Acetate - Run 1		
194.8	24.0	13,170	315	.222
195.4	24.6	11,820	288	.208
195.7	24.9	11,300	245	.228
196.0	25.2	10,880	245	.215
196.4	25.6	10,220	230	.207
		Ethyl Acetate - Run 2		
196.8	26.0	14,780	292	.270
199.3	28.5	14,130	296	.242
199.9	29.1	12,640	253	.239
200.0	29.2	12,220	230	.250
200.1	29.3	11,570	218	.242
200.2	29.4	10,760	182.9	.256
200.3	29.5	10,120	182.9	.232
200.2	29.4	9,090	171.2	.206

TABLE I (Continued)

T_{FW}, ^oF	T_{FX}, ^oF	Q/A, Btu/hr-ft^2	N, Sites/in^2	Q_n/n Btu/hr-site
		Ethyl Acetate - Run 2 (Continued)		
200.2	29.4	8,470	136.2	0.228
200.2	29.4	8,340	116.8	.258
200.2	29.4	7,560	116.8	.212
200.2	29.4	6,810	89.5	.218
200.0	29.2	5,610	62.3	.184
199.8	29.0	5,160	35.0	.244
198.8	28.0	4,180	7.8	.374
		Ethyl Acetate - Run 3		
201.0	30.2	13,780	249	.269
201.3	30.5	12,920	249	.246
201.4	30.6	11,820	210	.252
201.4	30.6	10,870	194.6	.238
201.4	30.6	10,760	179.0	.254
201.4	30.6	9,620	136.2	.276
201.4	30.6	9,290	128.4	.274
201.4	30.6	8,540	109.0	.276
201.4	30.6	8,010	105.1	.251
201.2	30.4	6,860	58.4	.320
201.1	30.3	5,910	38.9	.314
200.5	29.7	5,310	19.5	.454
199.8	29.0	4,190	7.8	.232
		Ethyl Acetate - Run 4		
202.0	31.2	13,420	257	.246
202.2	31.4	12,280	234	.236
202.3	31.5	11,720	206	.248
202.4	31.6	11,020	175.2	.264
202.4	31.6	10,370	179.0	.233
202.4	31.6	9,200	132.2	.254
202.4	31.6	8,700	109.0	.276
202.3	31.5	8,140	93.4	.281
202.2	31.4	7,300	73.9	.278
202.1	31.3	6,590	58.4	.270
201.6	30.8	5,750	42.8	.247
		Ethylene Dichloride - Run 1		
207.8	25.5	14,770	311	.254
207.7	25.4	14,020	288	.257

TABLE I (Continued)

T_w, °F	T_x, °F	Q/A, Btu/hr-ft^2	N, Sites/in^2	Q_n/n Btu/hr-site
		Ethylene Dichloride – Run 1 (Continued)		
207.5	25.2	13,410	284	0.246
207.0	24.7	12,230	253	.247
206.8	24.5	11,580	253	.230
206.6	24.3	10,820	253	.210
206.4	24.1	10,230	237	.207
205.9	23.6	9,880	210	.225
205.8	23.5	9,430	214	.207
205.4	23.1	8,860	190.7	.214
205.1	22.8	8,270	159.6	.232
204.7	22.4	7,620	163.3	.202
204.3	22.0	7,010	144.0	.202
204.1	21.8	6,640	136.2	.196
202.9	20.6	5,860	112.8	.200
202.6	20.3	5,520	101.2	.205
202.1	19.8	4,960	93.4	.185
201.4	19.1	4,380	74.0	.189
199.9	17.6	3,700	62.3	.175
198.3	16.0	3,000	46.7	.167
198.0	15.7	2,690	27.2	.220
		Ethylene Dichloride – Run 2		
210.2	27.9	17,460	–	
209.5	27.2	15,280	296	.273
208.9	26.6	13,530	280	.247
208.4	26.1	11,980	245	.232
207.8	25.5	10,320	234	.206
206.9	24.6	8,640	194.6	.193
206.5	24.2	7,770	186.8	.171
206.1	23.8	7,210	132.2	.216
205.8	23.5	7,030	140.2	.197
205.4	23.1	6,260	109.0	.208
204.5	22.2	5,020	73.9	.204
203.3	21.0	4,410	62.3	.194
202.2	19.9	3,640	42.8	.188
198.9	16.6	2.685	19.5	.252
		Ethylene Dichloride – Run 3		
209.4	27.1	14,180	284	.258
208.7	26.4	12,020	261	.226
208.3	26.0	10,180	198.3	.235

TABLE I (Continued)

T_w, °F	T_x, °F	Q/A, Btu/hr-ft²	N, Sites/in²	Q_n/n Btu/hr-site

Ethylene Dichloride – Run 3 (Continued)

207.4	25.1	8,660	179.0	0.207
207.0	24.7	7,980	147.8	.223
206.9	24.6	7,580	147.8	.204
206.4	24.1	6,090	101.2	.201
204.8	22.5	4,870	62.3	.222
205.5	23.2	5,020	62.3	.228
203.5	21.2	3,940	35.0	.250
202.0	19.7	3,220	23.4	.226

Cyclohexane – Run 1

200.6	22.1	14,180	–	
198.8	20.3	10,640	323	.170
198.0	19.5	9,140	284	.160
197.4	18.9	8,030	280	.137
196.8	18.3	7,140	241	.137
196.5	18.0	6,720	245	.124
195.7	17.2	5,760	202	.121
195.2	16.7	5,090	198.4	.103
194.4	15.9	4,380	155.7	.105
193.6	15.1	3,670	128.4	.097
192.5	14.0	2,910	89.5	.093
191.4	12.9	2,320	58.4	.094
189.8	11.3	1,690	23.4	.116

Cyclohexane – Run 2

200.0	21.5	12,830	–	
199.4	20.9	11,320	339	.175
198.8	20.3	10,180	323	.160
198.3	19.8	9,240	311	.147
197.6	19.1	8,190	284	.138
197.4	18.9	7,840	272	.136
196.9	18.4	7,180	272	.122
196.5	18.0	6,270	234	.116
196.0	17.5	5,840	202	.123
195.5	17.0	5,360	206	.107
194.6	16.1	4,760	175.2	.107
193.9	15.4	4,190	144.0	.109
193.5	15.0	3,750	105.2	.125
192.7	14.2	2,970	85.6	.100
192.2	13.7	2,500	58.4	.099
191.0	12.5	2,100	38.9	.111

TABLE I (Continued)

T_w, $^\circ F$	T_x, $^\circ F$	Q/A, $Btu/hr\text{-}ft^2$	N, $Sites/in^2$	Q_n/n $Btu/hr\text{-}site$
		Trichloroethylene - Run 1		
222.4	34.0	19,780	-	
223.0	34.6	16,980	343	0.252
223.0	34.6	14,920	308	.234
222.7	34.3	12,300	272	.199
222.2	33.8	10,920	226	.200
222.0	33.6	10,090	182.9	.217
221.5	33.1	9,050	163.4	.202
221.4	33.0	8,600	136.2	.221
221.0	32.6	7,840	116.8	.216
220.8	32.4	7,210	101.2	.209
220.3	31.9	6,480	77.9	.214
219.6	31.2	6,050	58.4	.214
219.0	30.6	5,370	38.9	.273
218.4	30.0	4,340	27.2	.153
		Trichloroethylene - Run 2		
223.8	35.7	16,390	335	.242
224.3	36.2	15,000	327	.215
224.4	36.3	13,630	272	.224
224.2	36.1	12,000	214	.233
224.2	36.1	11,370	198.4	.229
223.9	35.8	10,330	159.6	.242
223.8	35.7	8,880	128.4	.222
223.3	35.2	8,620	105.1	.261
222.4	34.3	7,860	81.7	.285
222.0	33.9	7,100	62.3	.297
221.0	32.9	5,770	42.8	.245
		Trichloroethylene - Run 3		
224.7	36.6	14,570	304	.221
225.0	36.9	13,440	280	.209
224.6	36.5	11,980	230	.214
224.5	36.4	11,120	202	.214
224.3	36.2	9,960	144.0	.246
223.8	35.7	9,080	112.8	.266
223.3	35.2	8,440	116.8	.225
222.8	34.7	7,970	93.4	.252
222.1	34.0	7,150	62.3	.300
220.6	32.5	6,310	46.7	.316

TABLE II. PHYSICAL PROPERTIES OF LIQUIDS AT THEIR NORMAL BOILING POINTS

Liquid	λ, Btu/lb	ρ_L, lb/ft^3	ρ_v, lb/ft^3	s, lb/ft	c_L, Btu/lb°F	μ, lb/ft hr	k_L, Btu/hr ft°F
Carbon Tetrachloride	83.6	73.0	0.346	0.001362	0.219	1.177	0.0852
Chloroform	106.2	87.4	0.285	0.001482	0.243	0.968	0.1000
1,1,1-Trichloroethane	103.7	77.8	0.308	0.001308	0.267	1.017	0.038
Benzene	169.7	50.5	0.1743	0.001454	0.463	0.767	0.1187
Ethylene Dichloride	139.2	69.3	0.222	0.001640	0.327	0.992	0.077
Cyclohexane	168.8	43.8	0.1872	0.001253	0.489	0.980	0.0605
Trichloroethylene	103.2	82.4	0.290	0.001304	0.342	0.839	0.0658

TABLE III. COMPARISON OF NUCLEATE BOILING EQUATIONS

Exponent on

Author	T_x °F	t_w °F	λ Btu/lb	ρ_L lb/ft³	ρ_v lb/ft³	s lb/ft	C_L Btu/lb°F	μ_L lb/ft hr	k_L Btu/hr ft°F	P_x lb/ft²	P lb/ft²	P_c lb/ft²	g ft/hr²	D ft	$\rho_L - \rho_v$ lb/ft³
Hughmark		1.618	-1.15		-1.385		0.945	-1.630		1.867	-0.202	0.202			2.27
McNelly	3.22		-2.22		-1.06	-1	2.22		1		1				1.06
Forster – Zuber	0.24		-0.24	0.49	-0.24	-0.5	0.45	-0.29	0.79	0.75					
Gilmour	3.33		-2.33	0.917	-2.33	-1.417	1.333	-1	2		2.83			-3.33	
Forster – Greif		1.25	-1.5	0.5	-1.5	-0.5	0.46	-0.29	0.79	2					
Levy	3	-1		2		-1	1		1						-1
Chang – Snyder	1	0.4	-0.8		-0.8	-1	0.4		1	1.4					0.4
Rohsenow	3		-2			-0.5	-2.1	-4.1	5.1				0.5		0.5
Nishikawa	3		-1	2	-1	-1	1		2		1				
Miyauchi – Ya gi	3.85		-2.85	2.85	-0.19		2.43	-0.42	-2.43						
This study	3.22	-2.46	-2.68	1.83	-3.09	0.846	4.06	6.86	0.388						

47

Nichrome-tipped Lead
to Electronic Relay

Teflon Stopcock

Heater

Pressure-control
Bulb

Manometer

Copper Leads

Platinum Lead to
Electronic Relay

Copper Cables
to D-C Generator

Boiler

Copper Lead Out of
Boiler to Variac

Copper Potential
Leads Out of Boiler
to Kelvin Bridge

Heat Transfer Surface,
Gold or Copper Wire

Auxiliary Heater
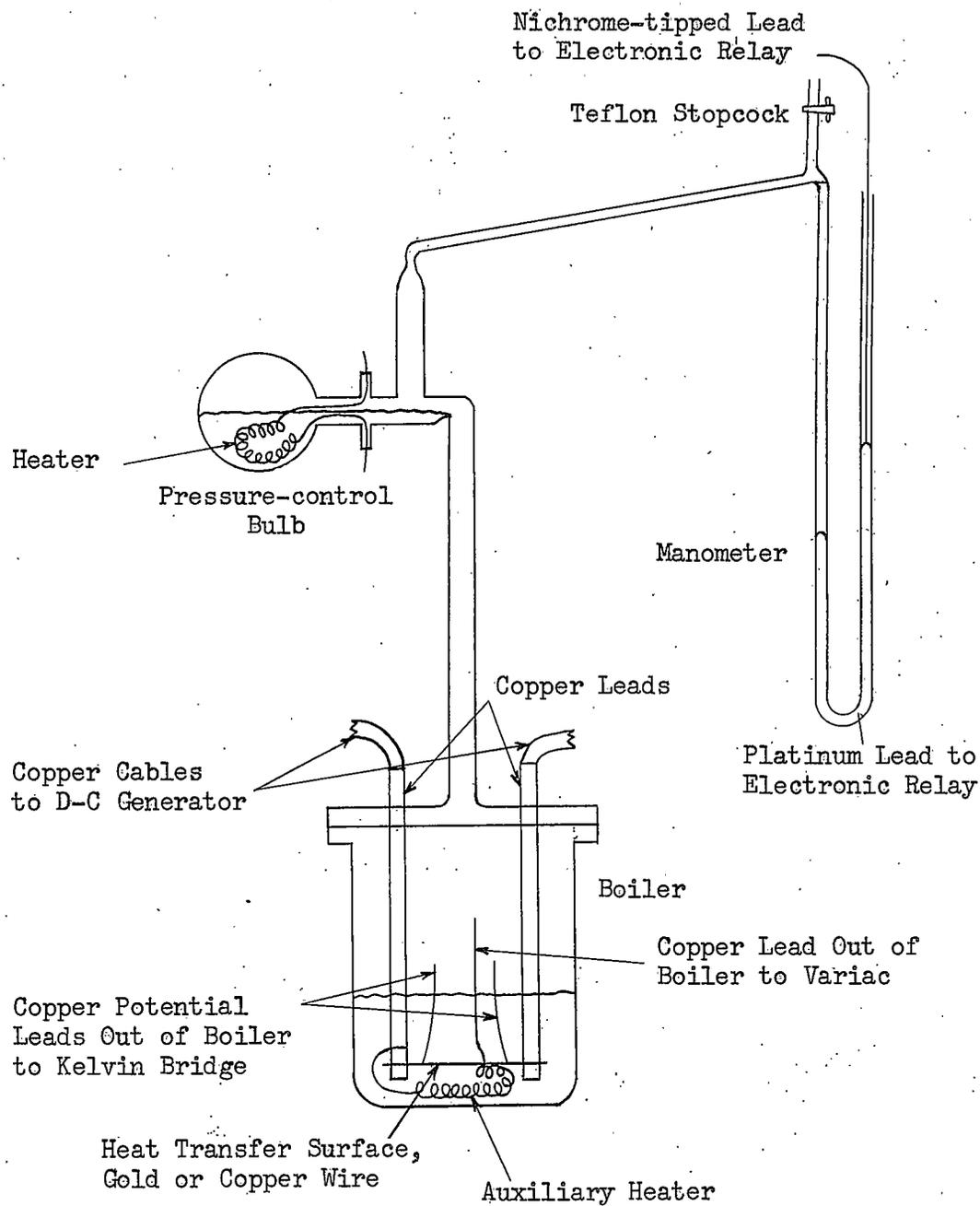
FIGURE 1. SIMPLIFIED DIAGRAM OF BOILING APPARATUS
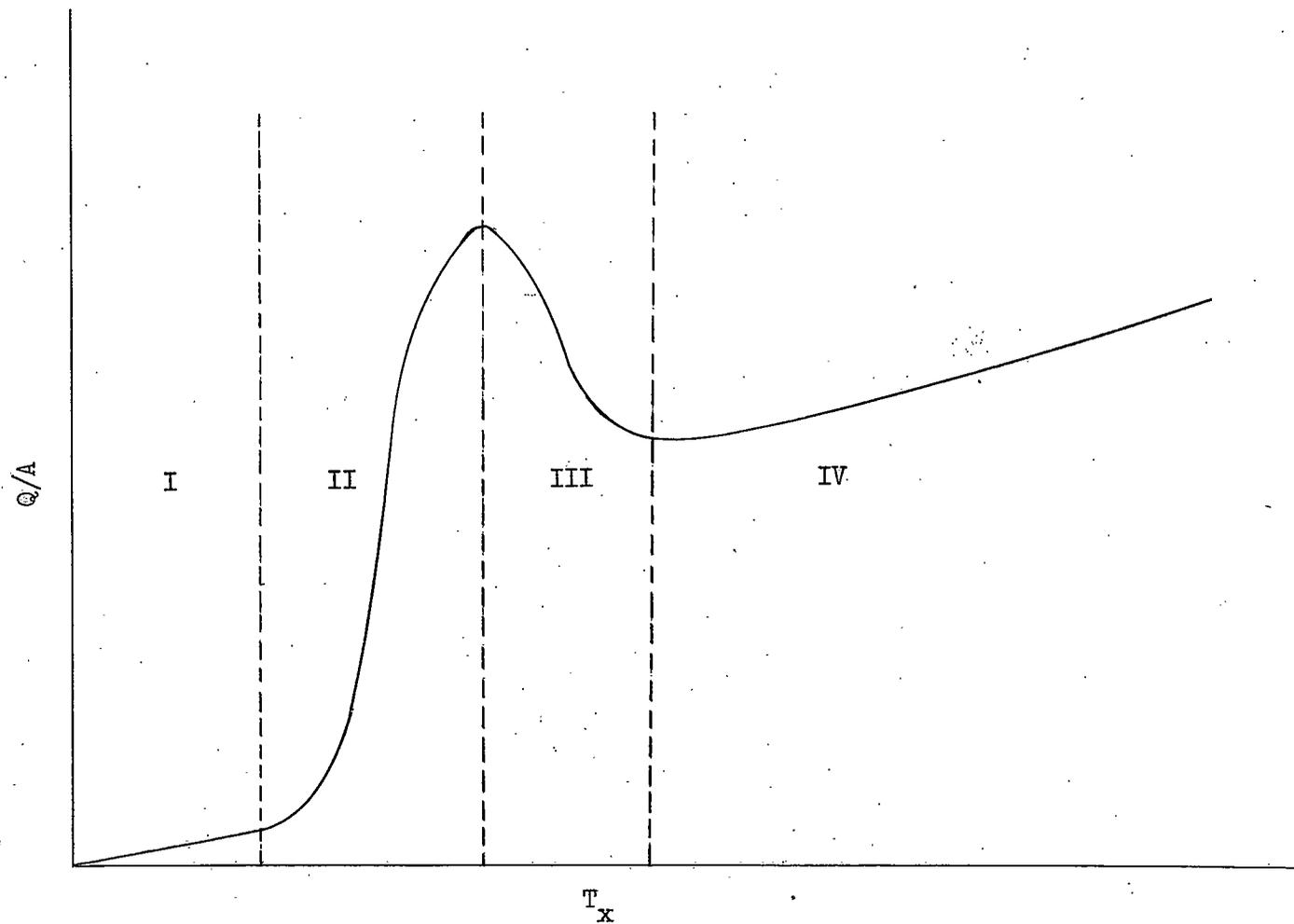
FIGURE 2. GENERAL BOILING CURVE
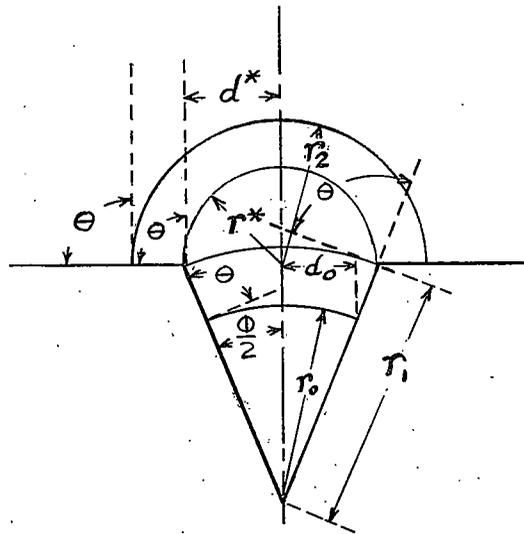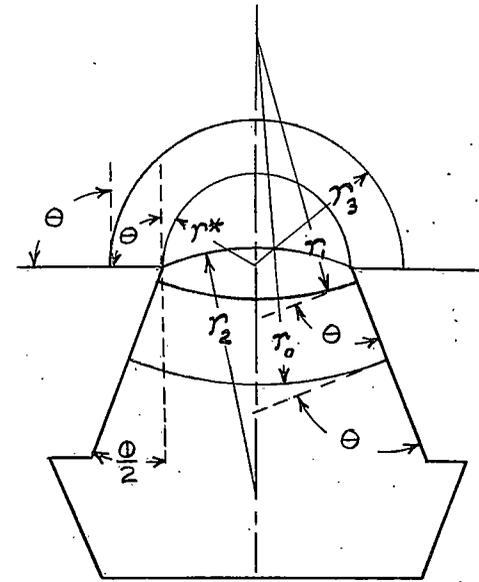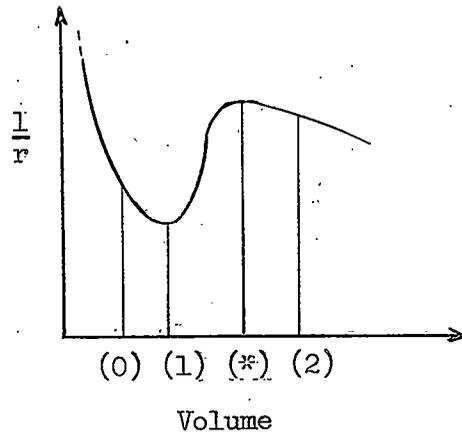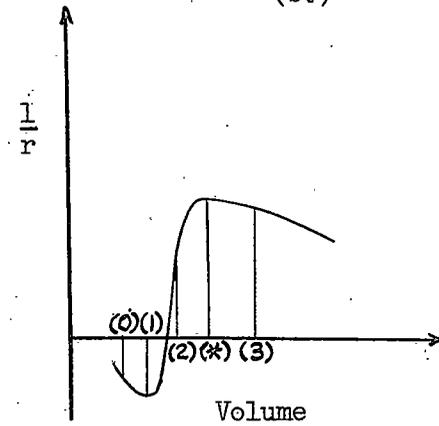
FIGURE 3. CAVITIES ACTING AS ACTIVE NUCLEATE BOILING SITES
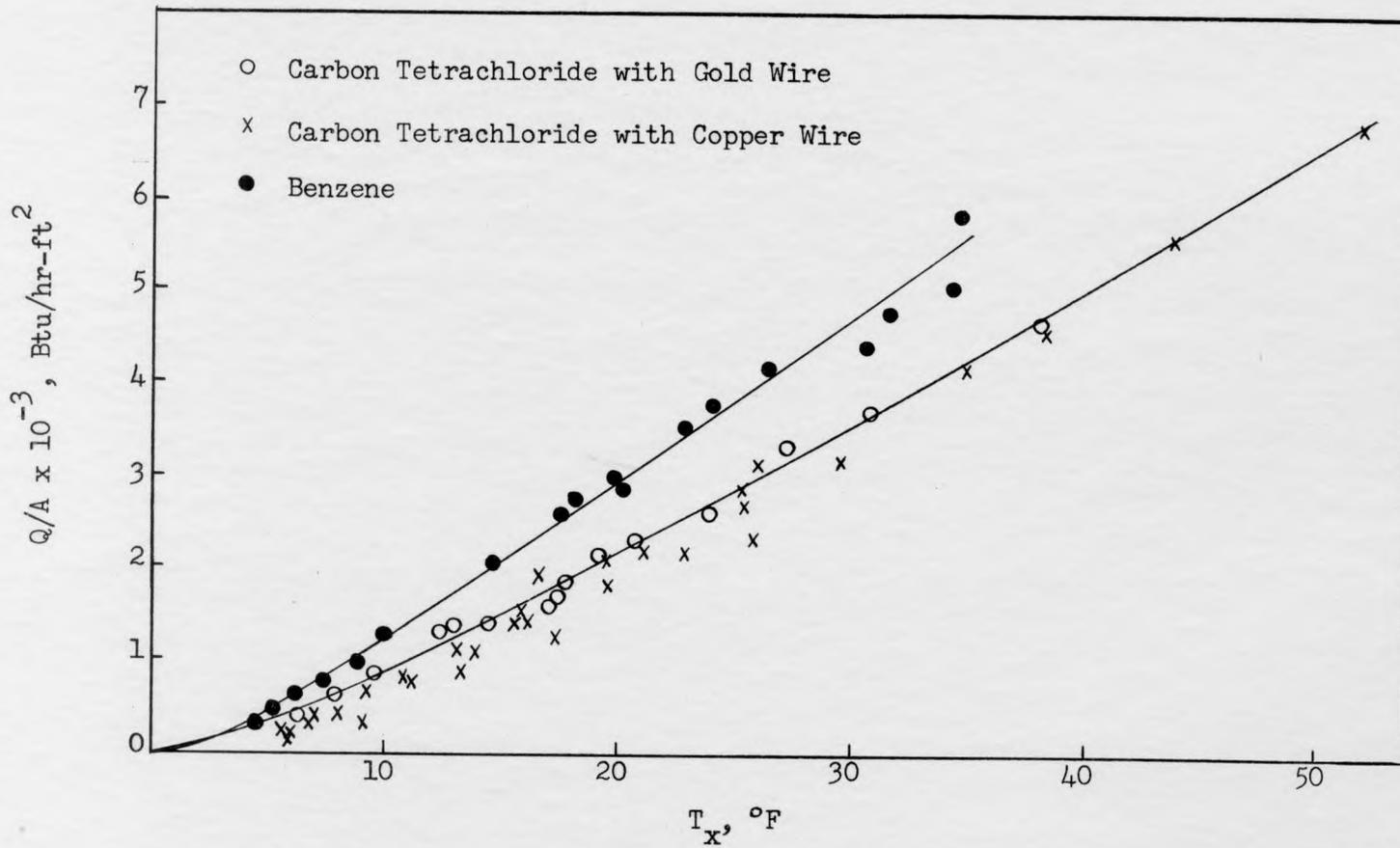
FIGURE 4. NATURAL CONVECTION CURVES, CARBON TETRACHLORIDE AND BENZENE
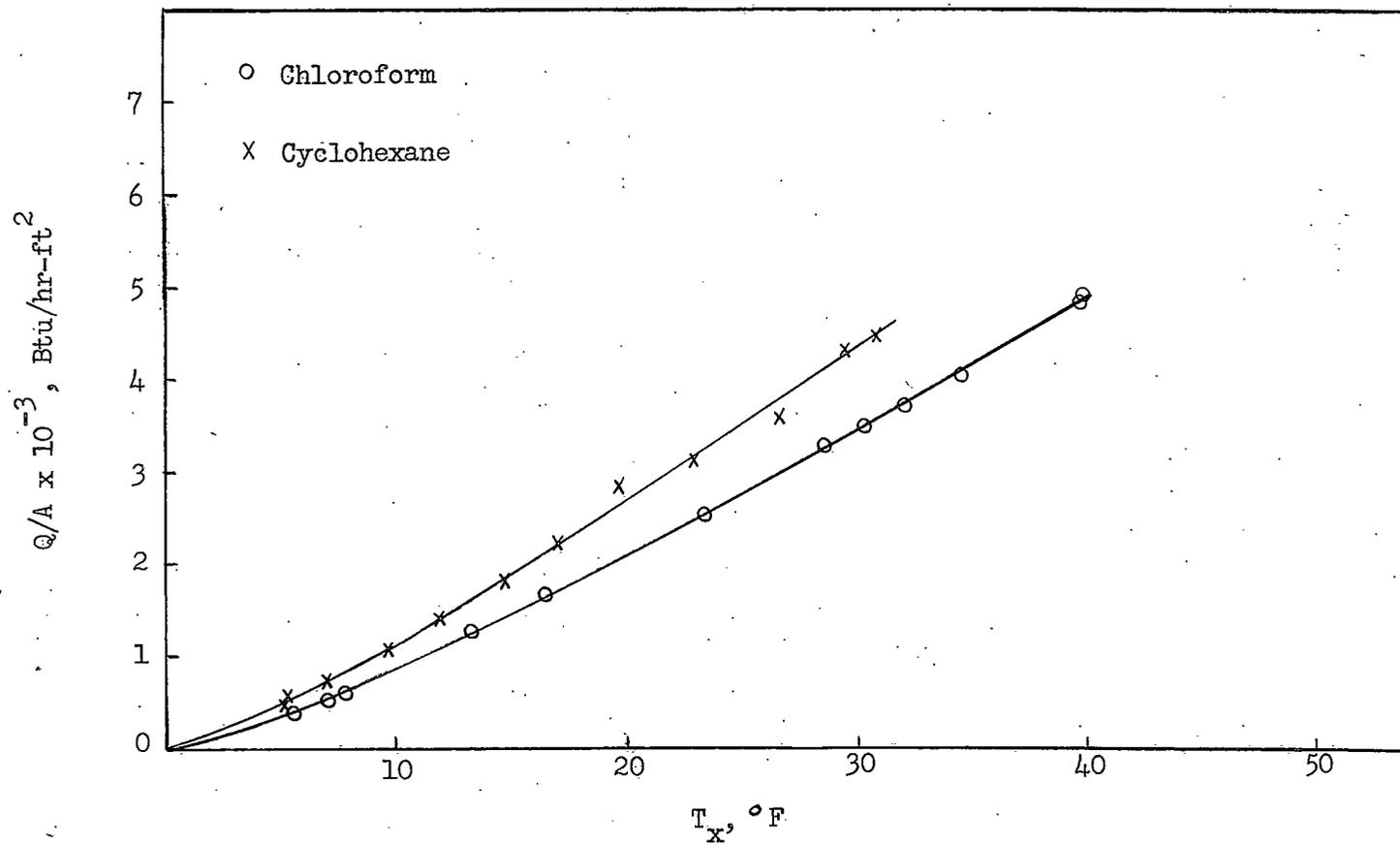
FIGURE 5. NATURAL CONVECTION CURVES, CHLOROFORM AND CYCLOHEXANE
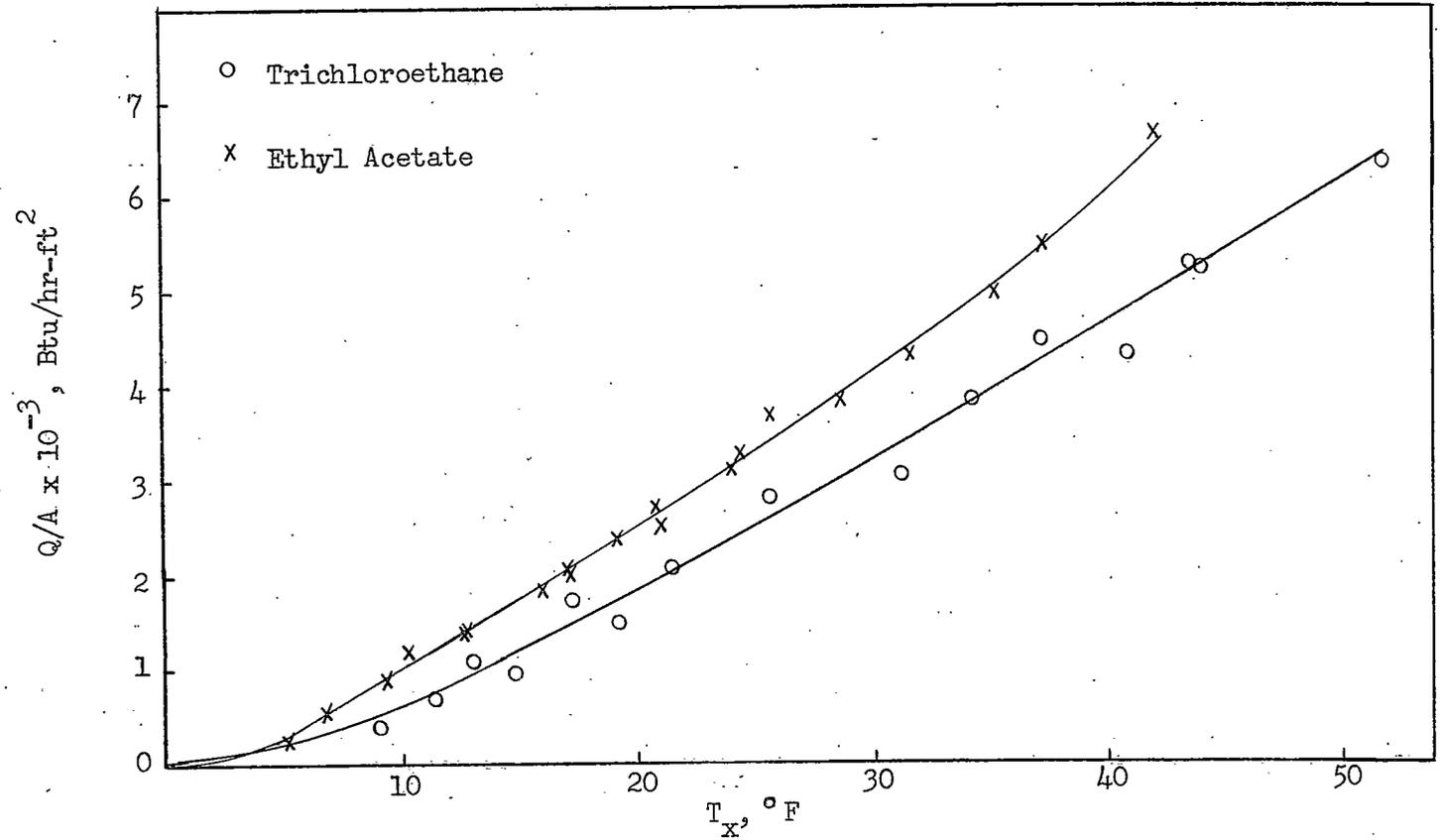
FIGURE 6. NATURAL CONVECTION CURVES, TRICHLOROETHANE AND ETHYL ACETATE
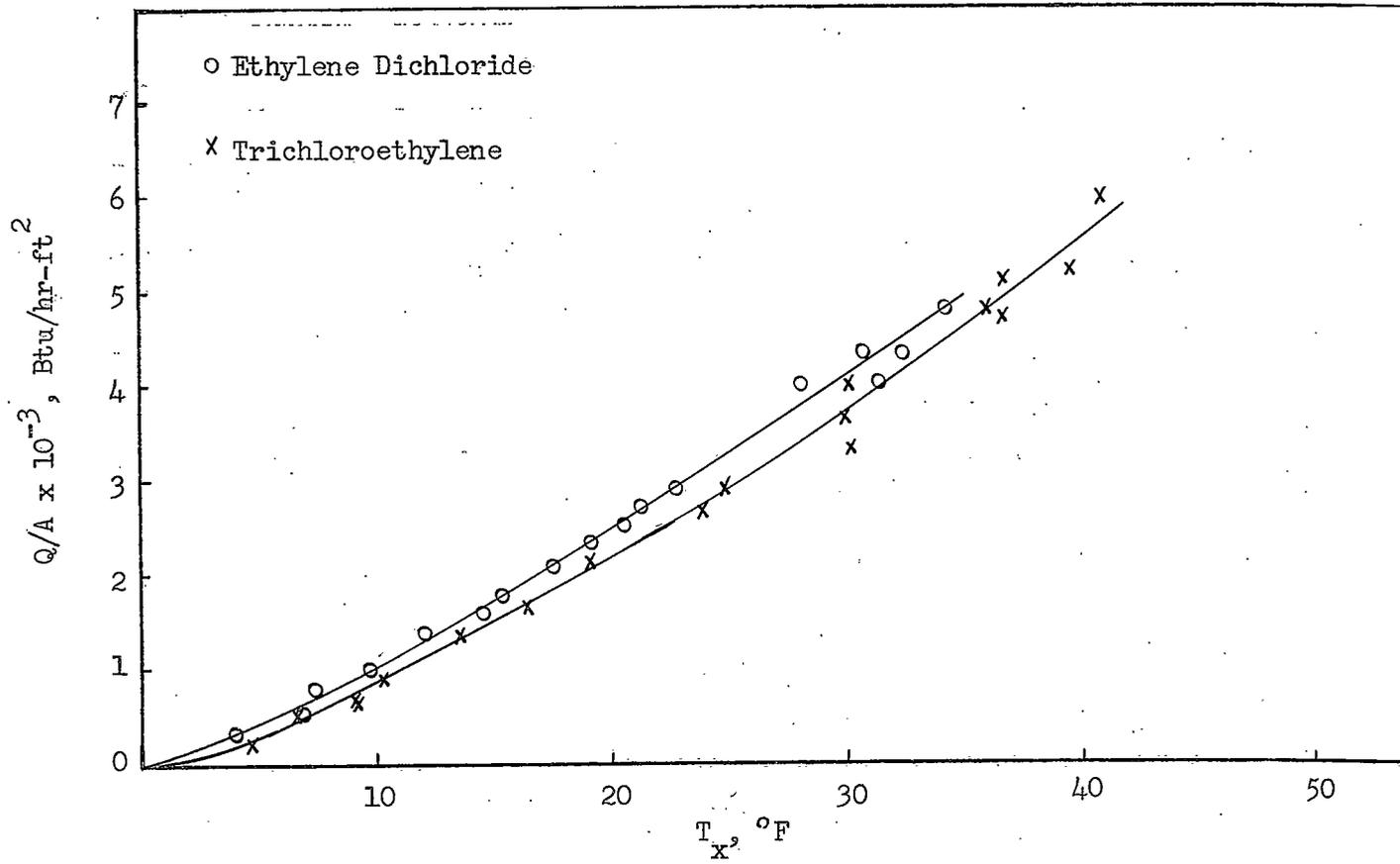
FIGURE 7. NATURAL CONVECTION CURVES, ETHYLENE DICHLORIDE AND TRICHLOROETHYLENE
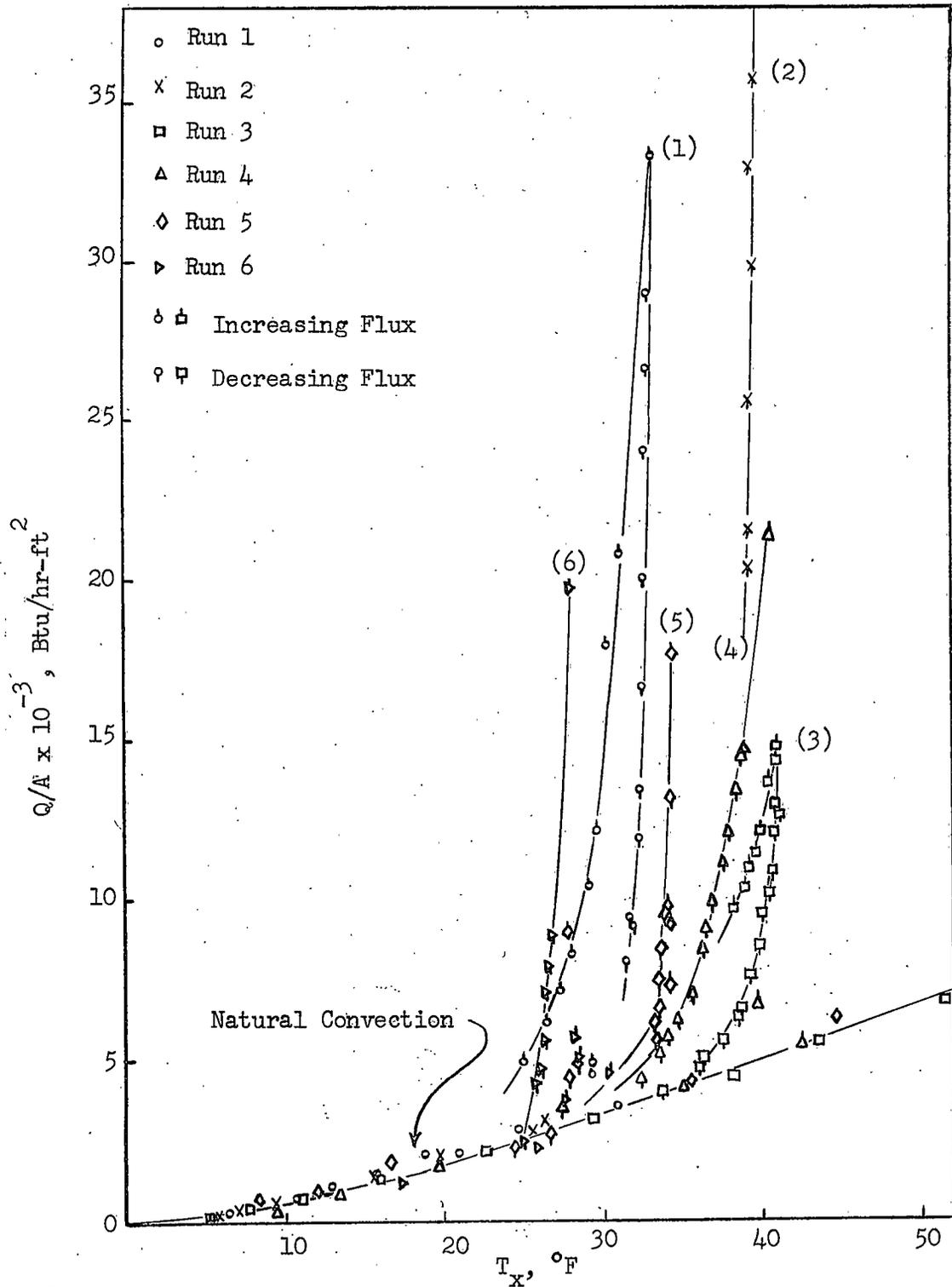
FIGURE 8. BOILING CURVES, CARBON TETRACHLORIDE WITH COPPER WIRES
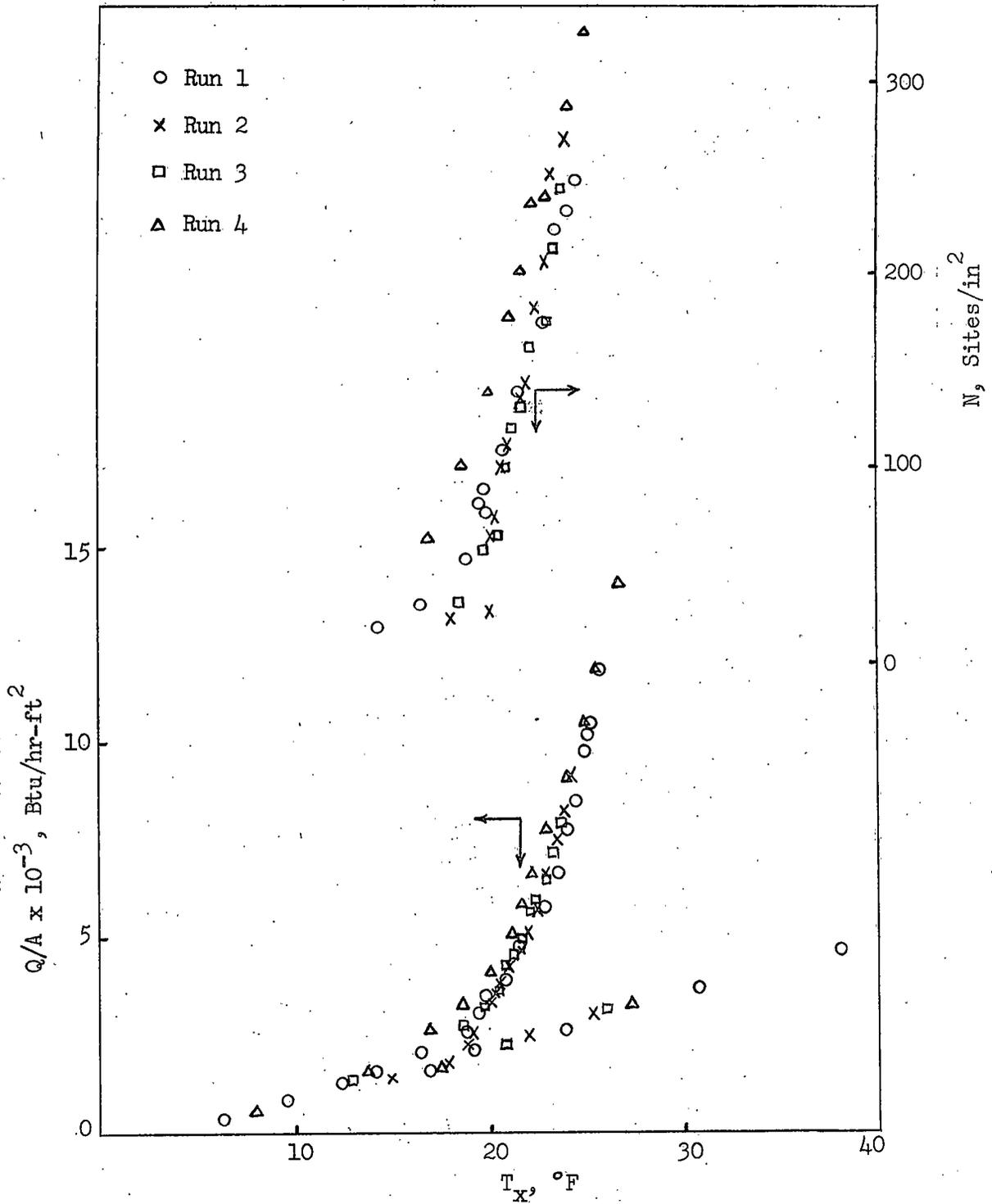
FIGURE 9. BOILING CURVES, CARBON TETRACHLORIDE WITH GOLD WIRE
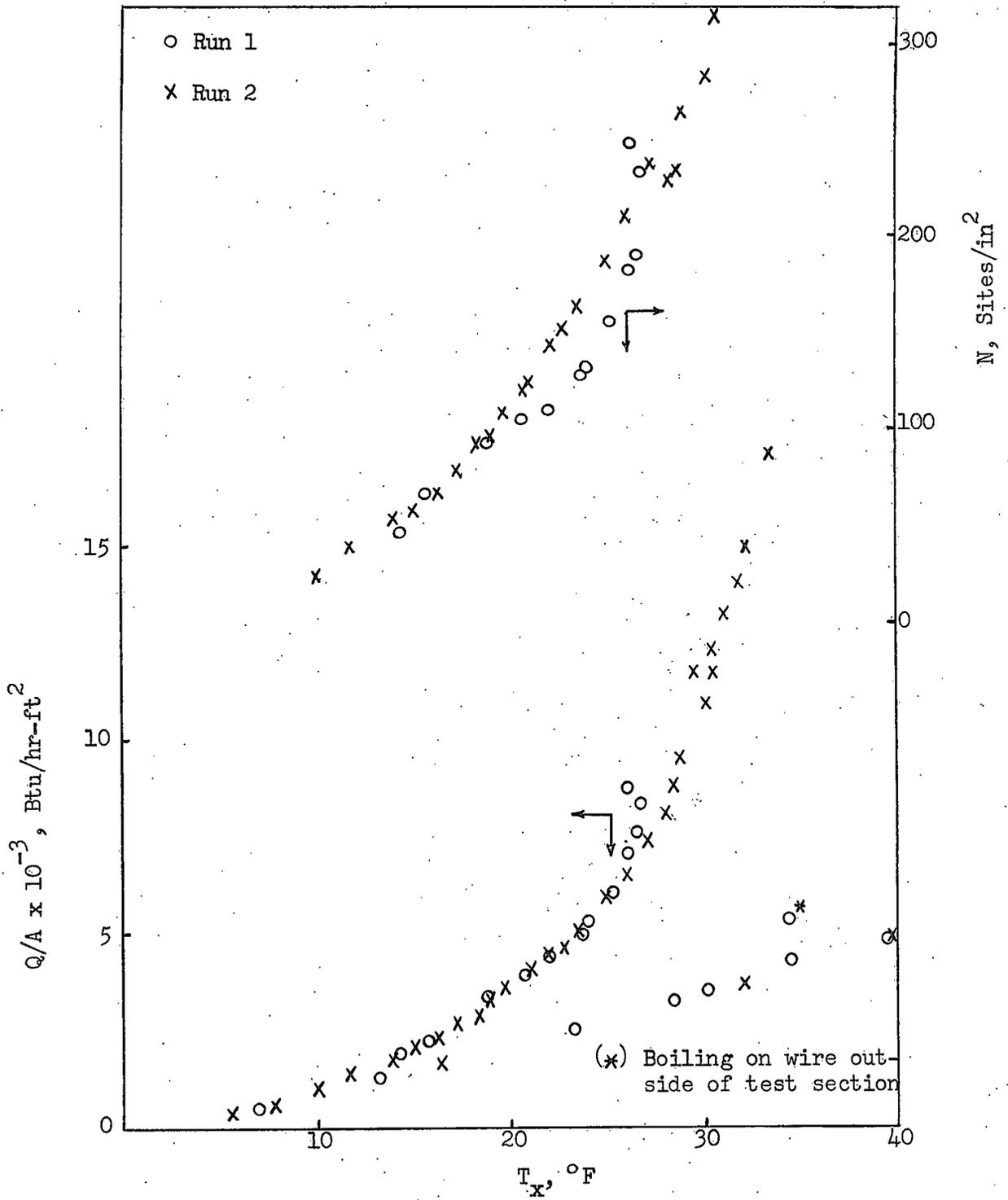
FIGURE 10. BOILING CURVES, CHLOROFORM WITH GOLD WIRE
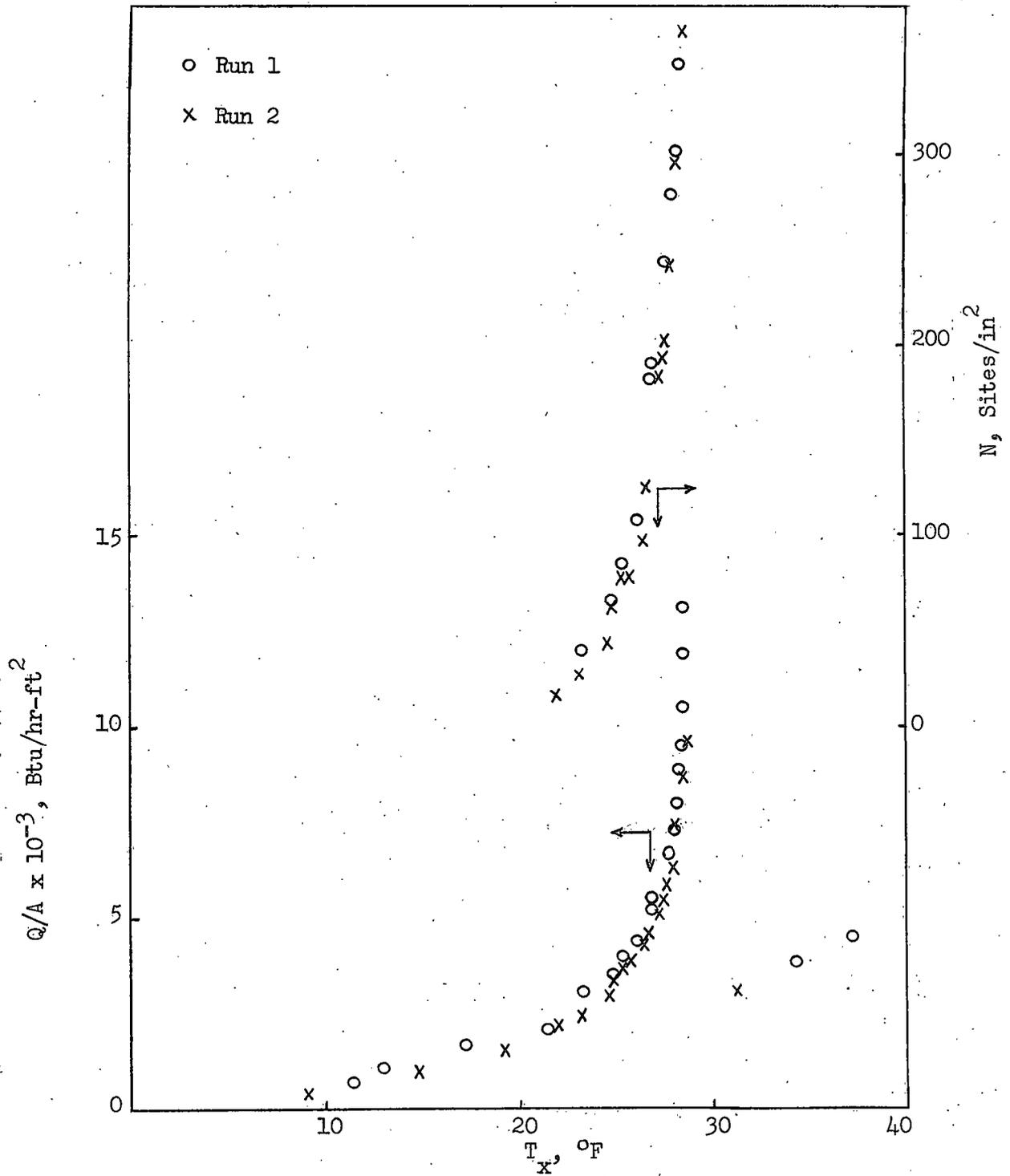
FIGURE 11. BOILING CURVES, TRICHLOROETHANE WITH GOLD WIRE
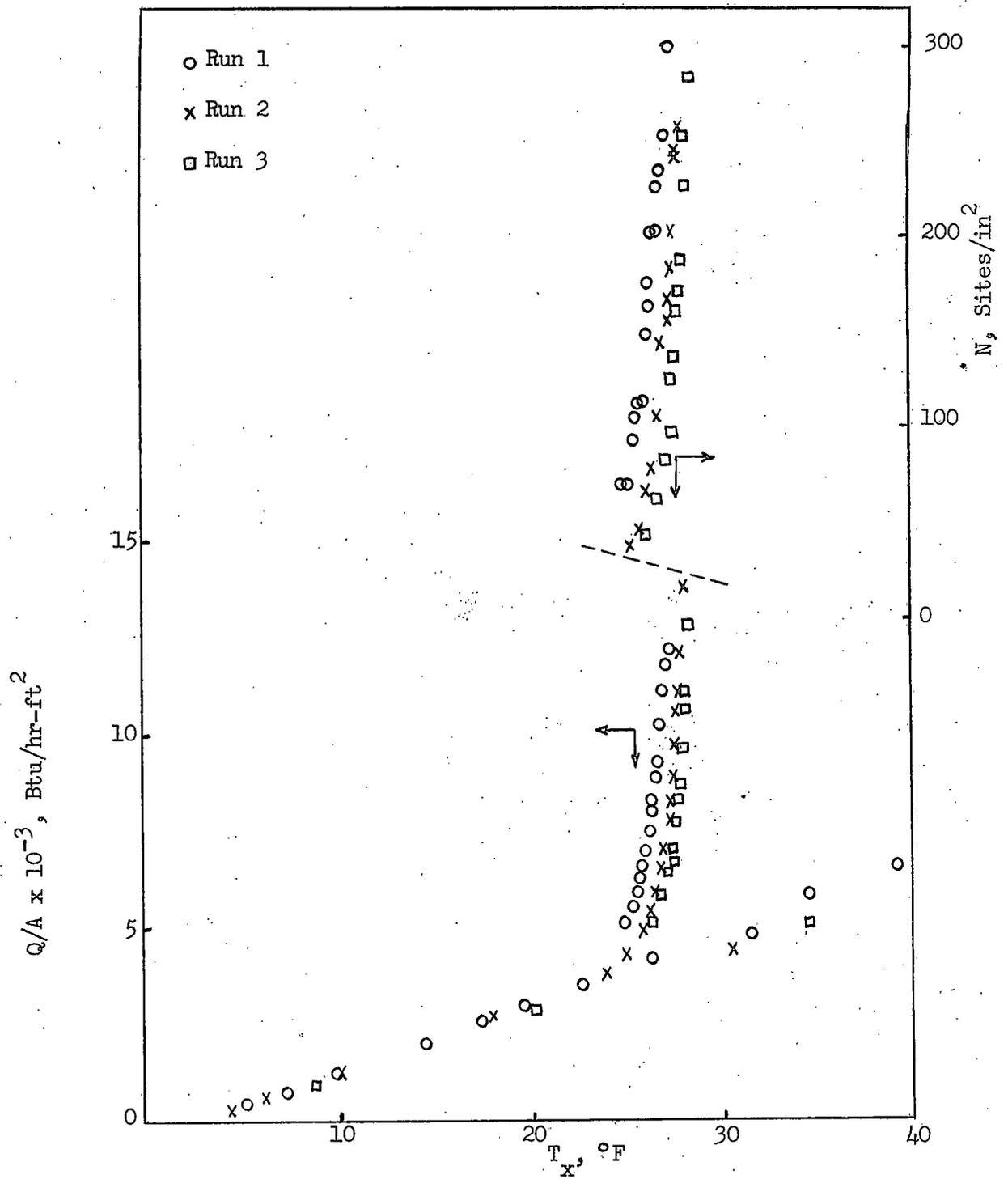
FIGURE 12. BOILING CURVES, BENZENE WITH GOLD WIRE
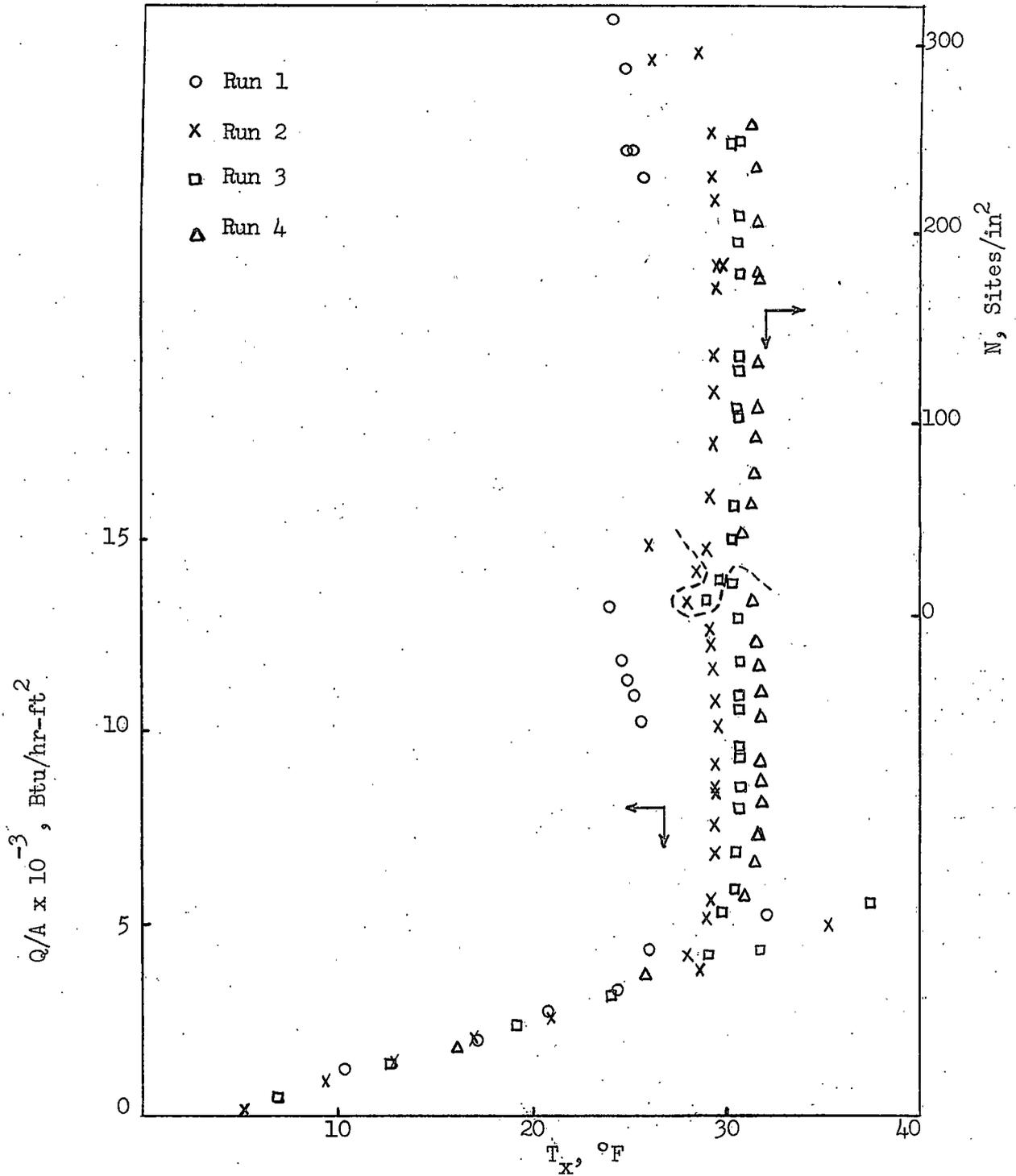
FIGURE 13. BOILING CURVES, ETHYL ACETATE WITH GOLD WIRE
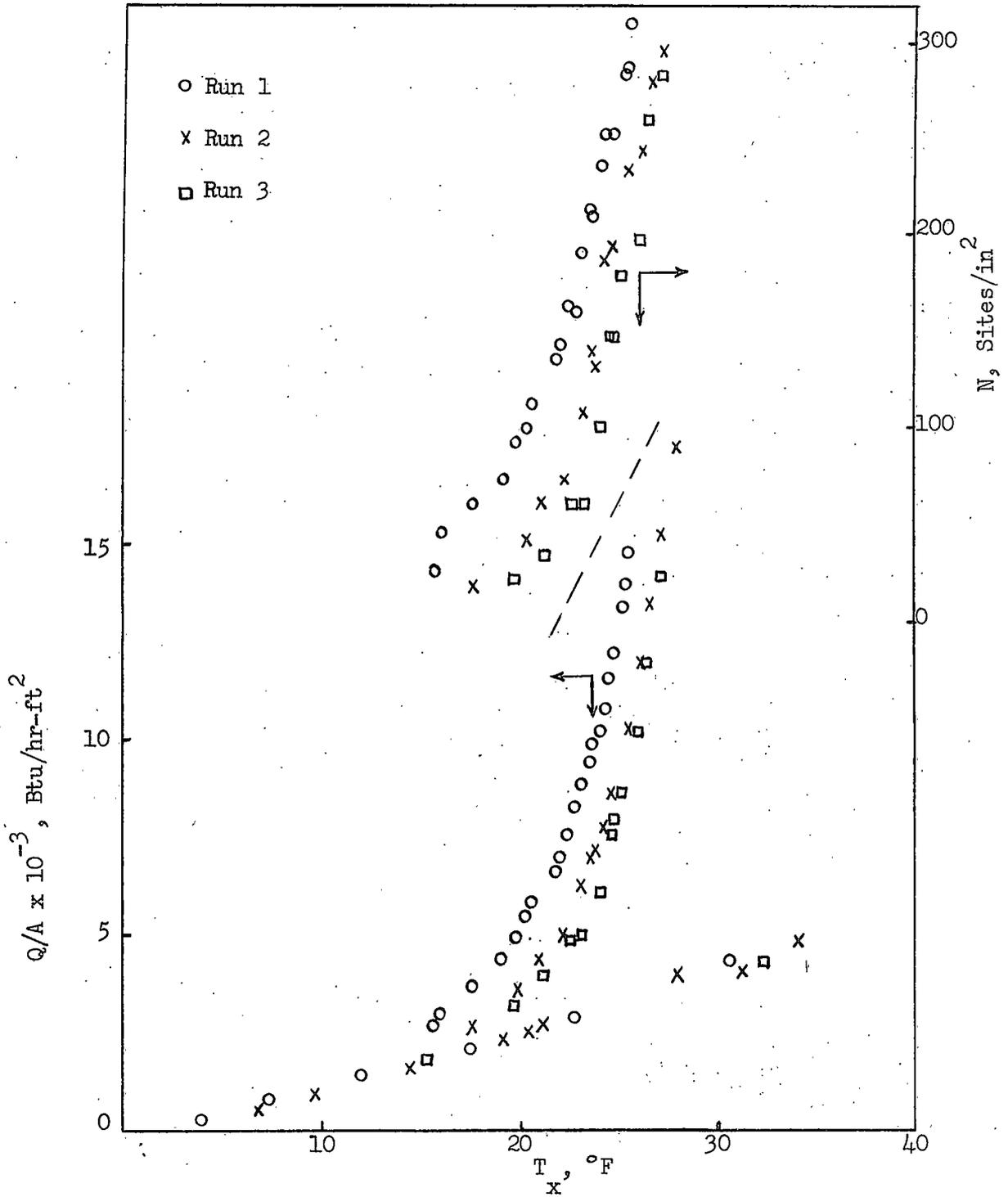
FIGURE 14. BOILING CURVES, ETHYLENE DICHLORIDE WITH GOLD WIRE
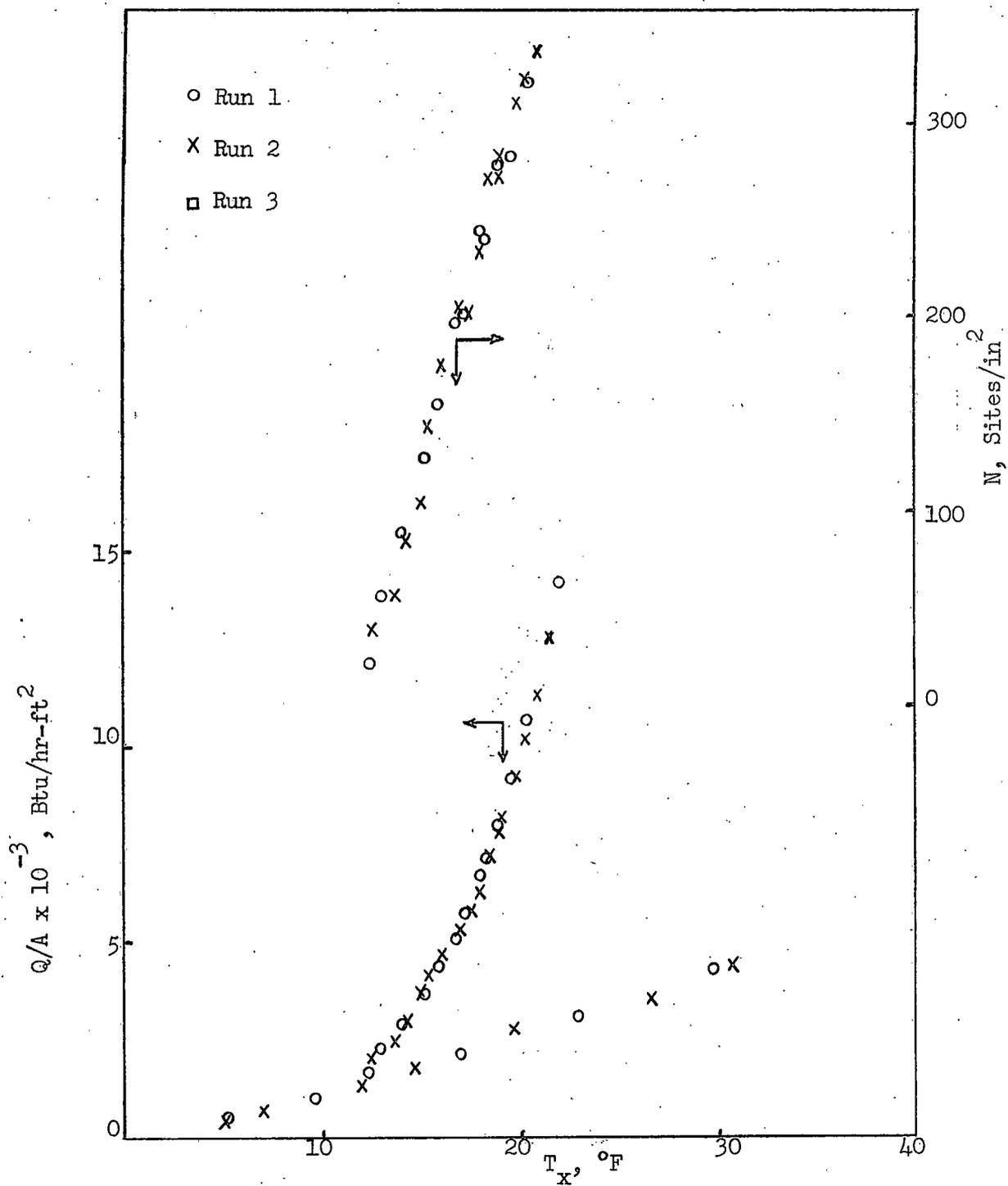
FIGURE 15. BOILING CURVES, CYCLOHEXANE WITH GOLD WIRE
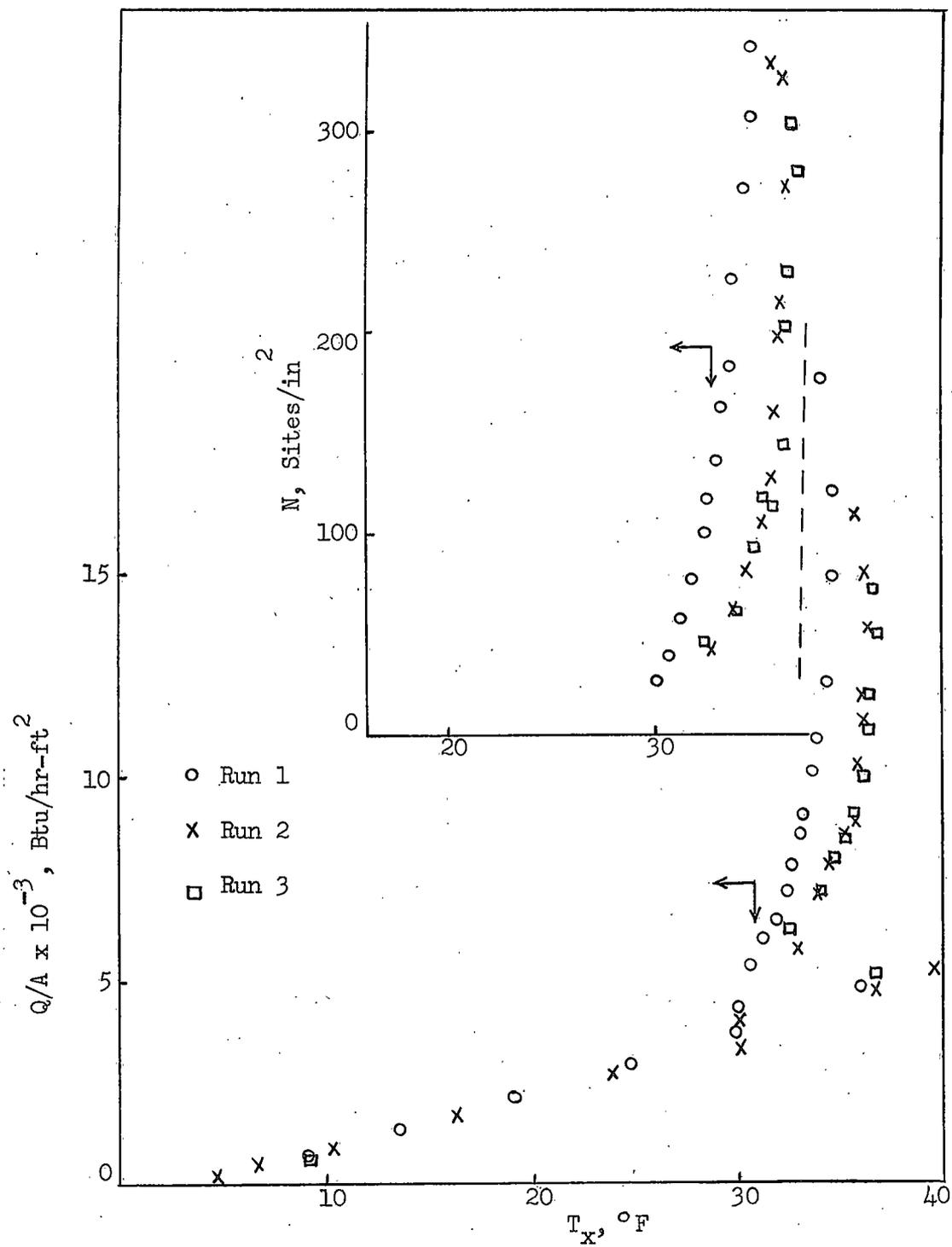
FIGURE 16. BOILING CURVES, TRICHLOROETHYLENE WITH GOLD WIRE
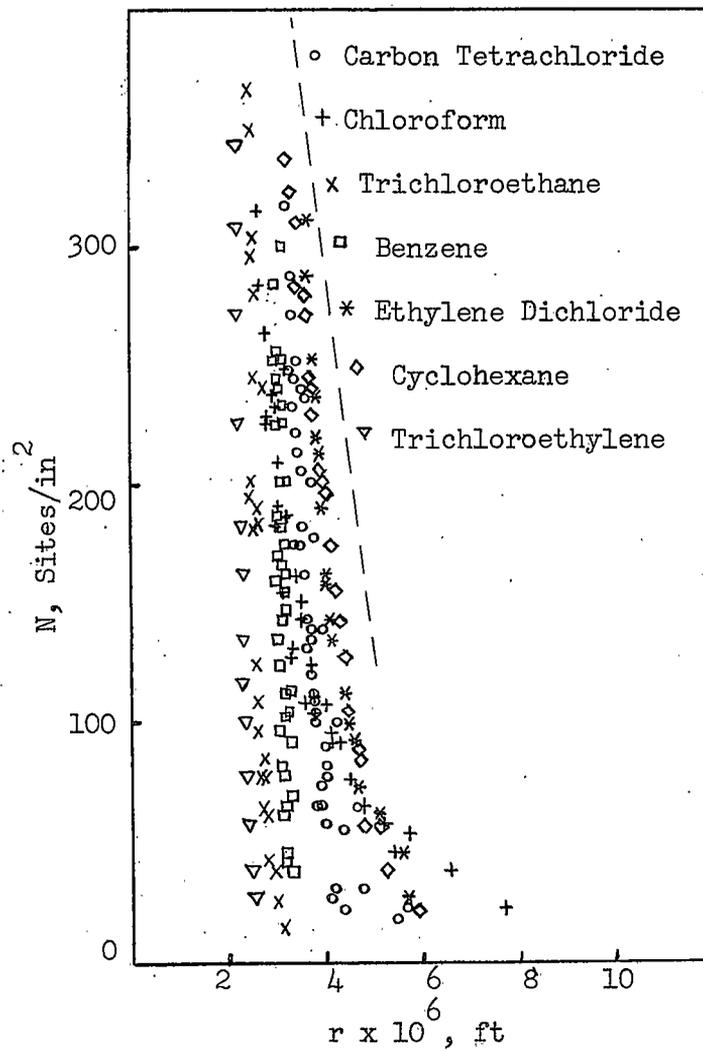
FIGURE 17. ACTIVE NUCLEATE SITE POPULATION VERSUS RADIUS
OF IDEAL CONICAL CAVITY
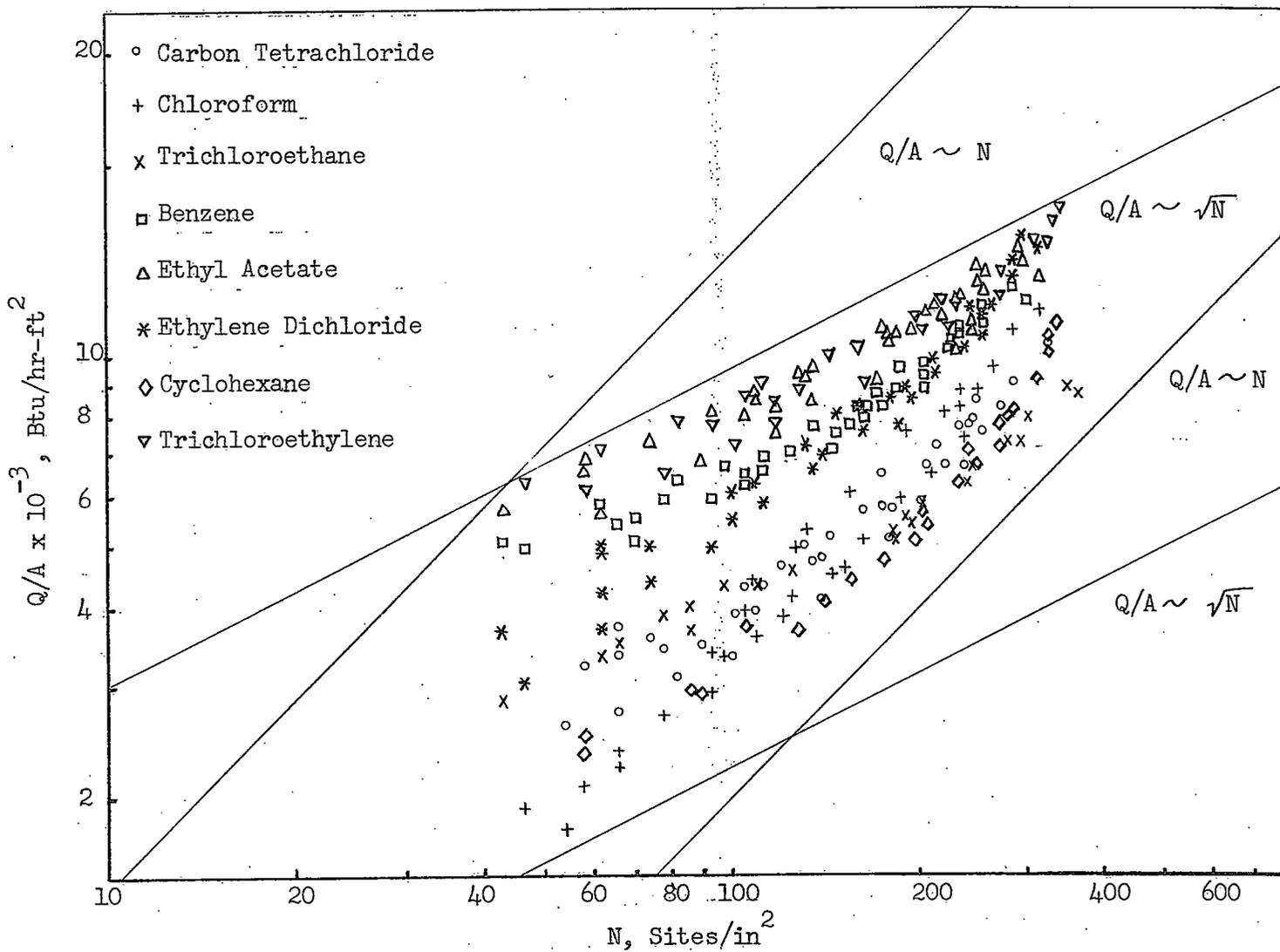
FIGURE 18. HEAT FLUX VERSUS ACTIVE NUCLEATE SITE POPULATION
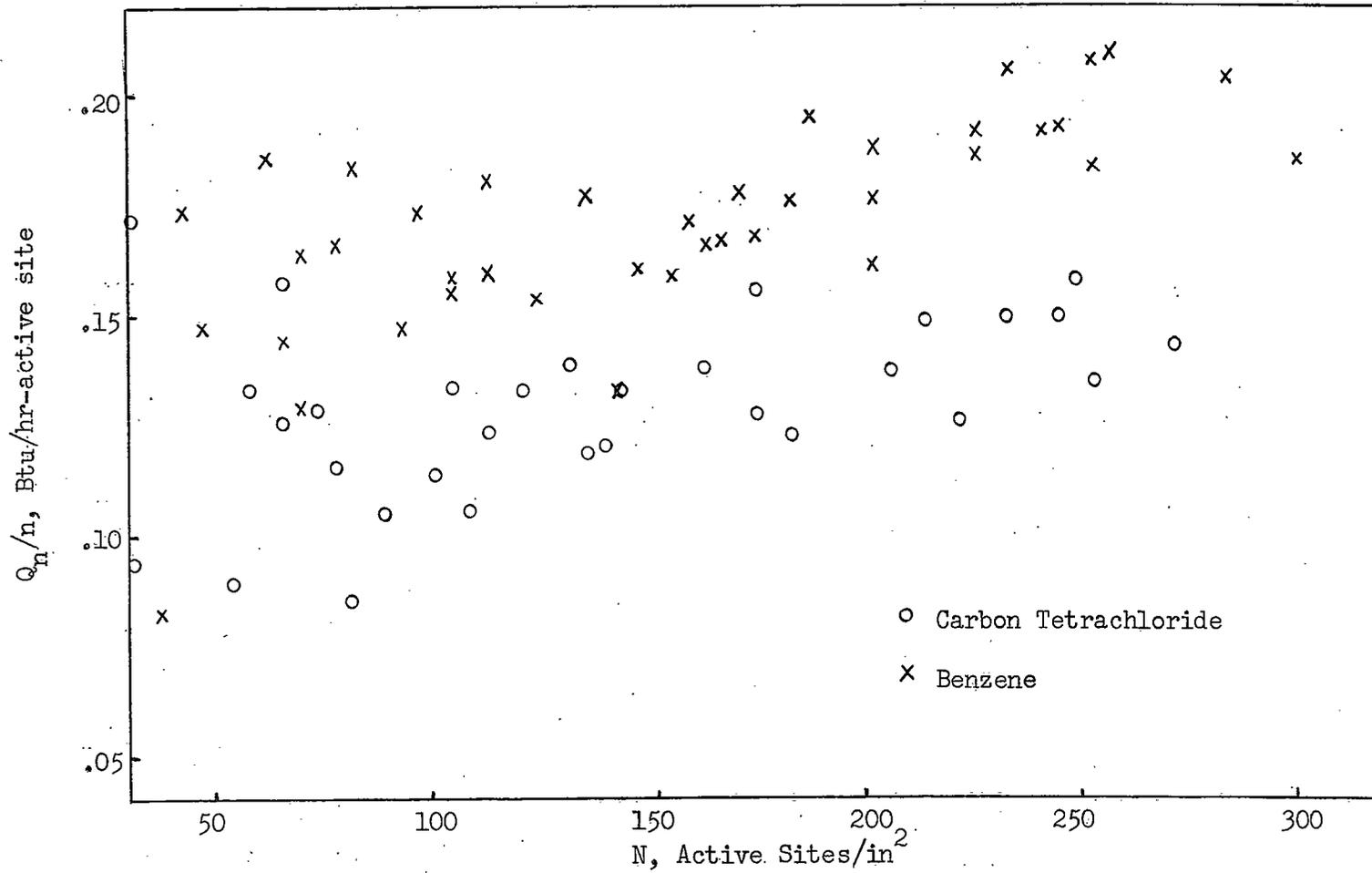
FIGURE 19. NUCLEATE HEAT TRANSFER RATE CONTRIBUTIONS, CARBON TETRACHLORIDE AND BENZENE

Y-axis: Q_n/n, Btu/hr-active site

X-axis: N, Active Sites/in^2

Legend:
O Carbon Tetrachloride
X Benzene
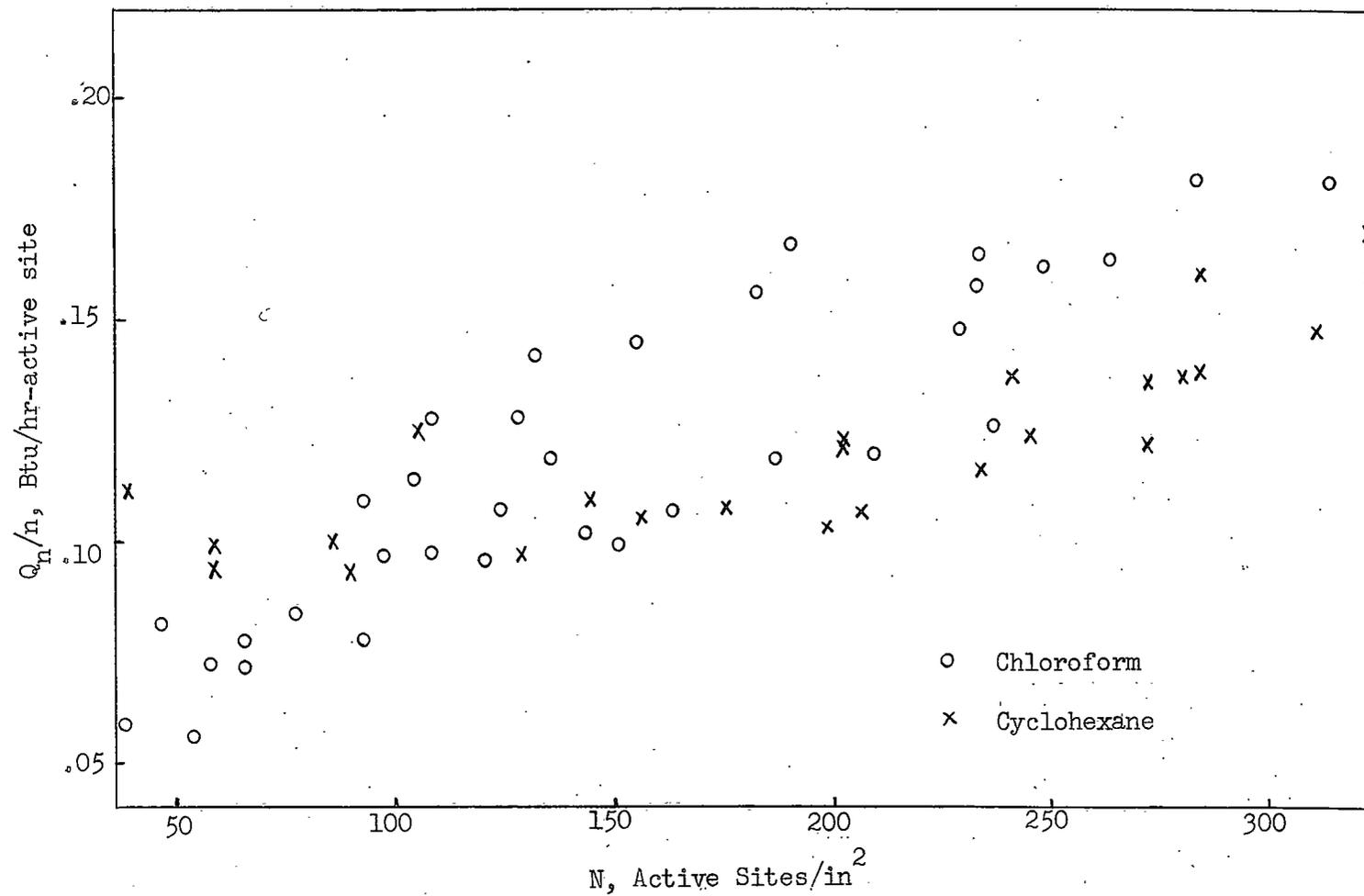
FIGURE 20. NUCLEATE HEAT TRANSFER RATE CONTRIBUTIONS, CHLOROFORM AND CYCLOHEXANE
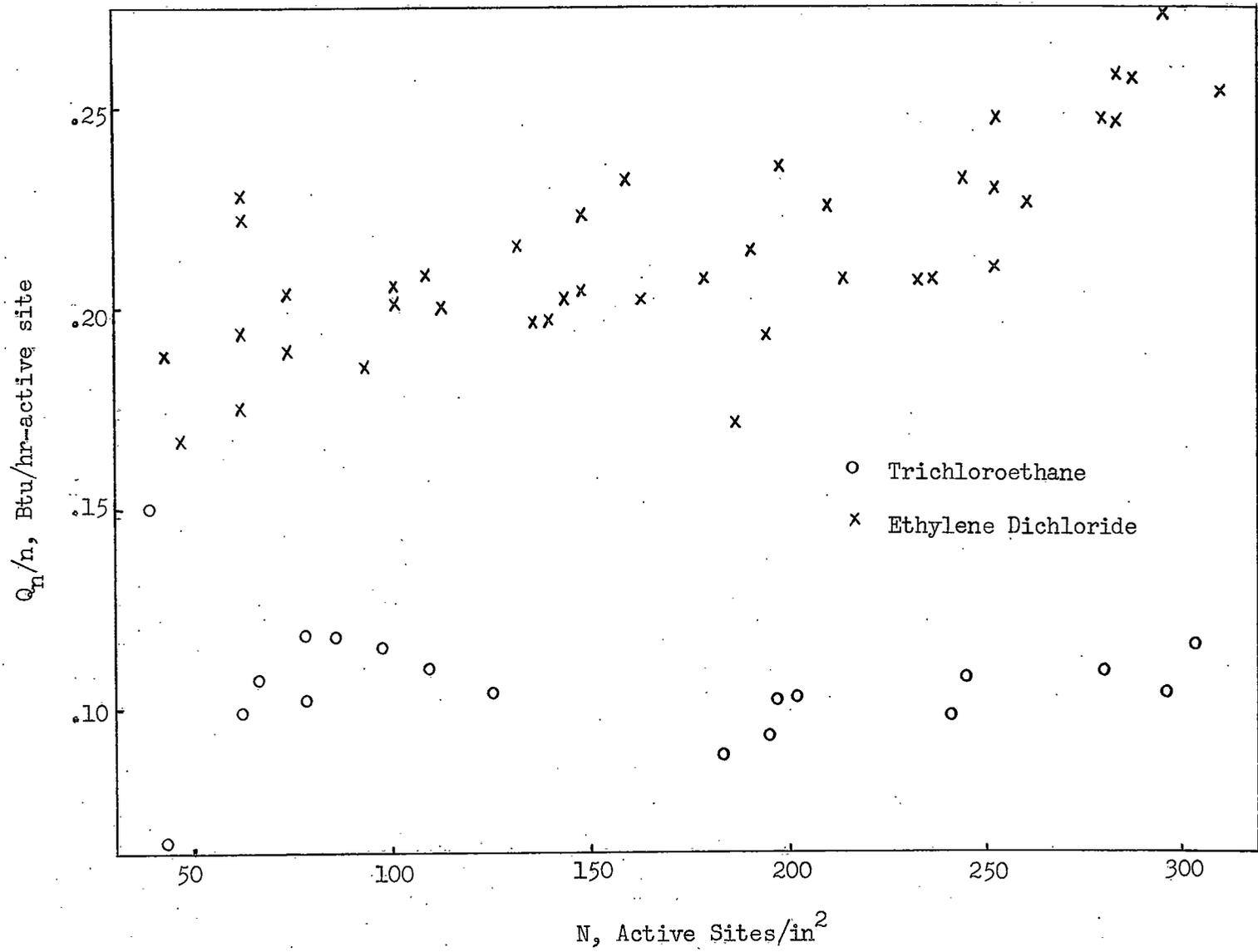
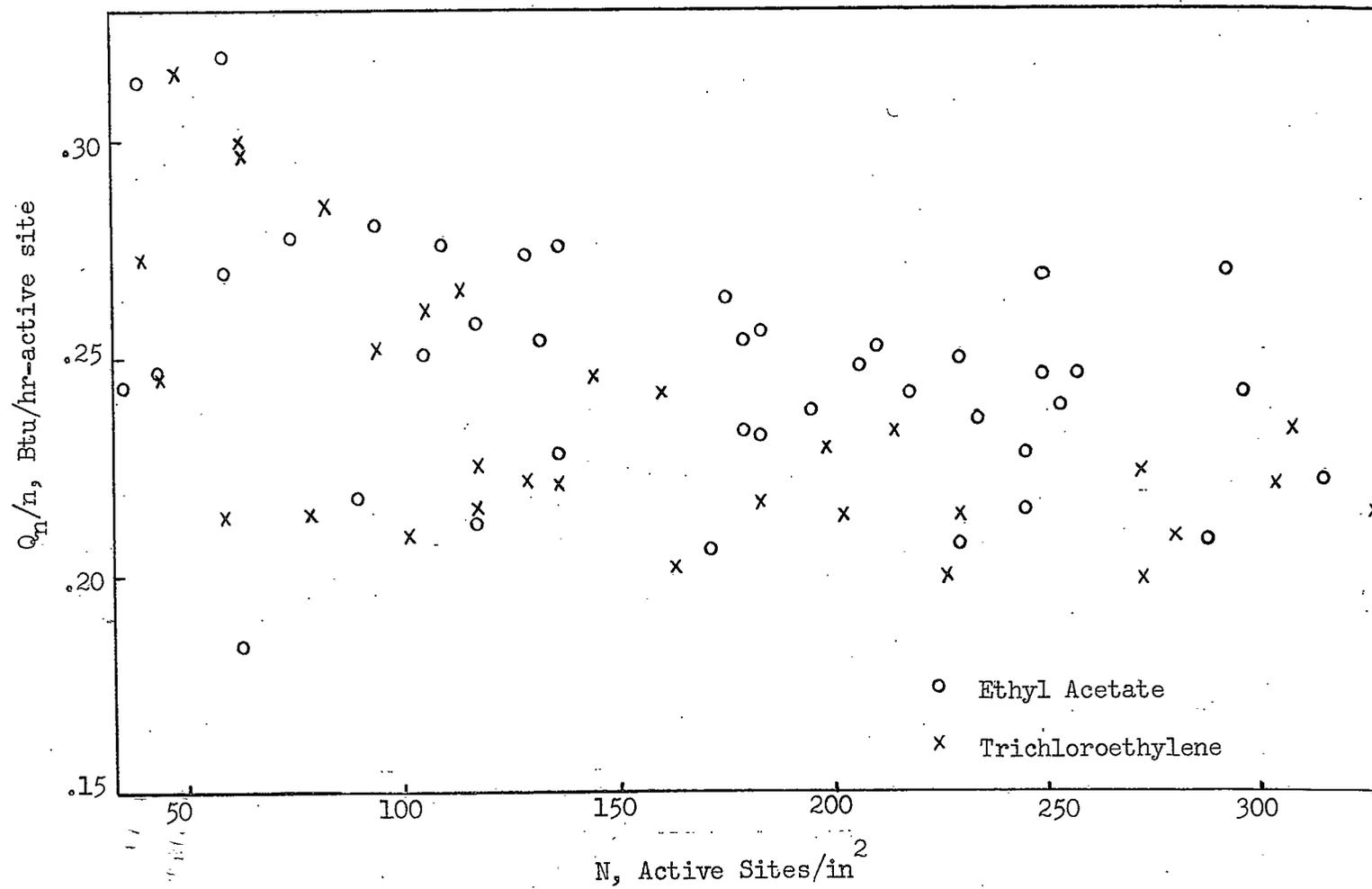FIGURE 21. NUCLEATE HEAT TRANSFER RATE CONTRIBUTIONS, TRICHLOROETHANE AND ETHYLENE DICHLORIDE

FIGURE 22. NUCLEATE HEAT TRANSFER RATE CONTRIBUTIONS, ETHYL ACETATE AND TRICHLOROETHYLENE

LITERATURE CITED

1. Bankoff, S. G., Am. Inst. Chem. Engrs. Meeting, May 6-9, New Orleans, La., Abstract No. 10, 1956

2. Bankoff, S. G., Heat Transfer and Fluid Mechanics Inst., pp. 1-13, Stanford University Press, Stanford, Calif., 1956

3. Brunk, H. D., *An Introduction to Mathematical Statistics*, Ginn and Co., Boston, 1960

4. Clark, H. B., Strenge, P. S., Westwater, J. W., "Active Sites for Nucleate Boiling," *Chem. Eng. Progress Symposium Series, 55*, No. 29 (1959) p. 103-110

5. Corty, Claude and Foust, Alan S., "Surface Variables in Nucleate Boiling," *Chem. Eng. Progress Symposium Series*, No. 17, Vol. 51, (1955) p. 1-12a

6. Crow, E. L., Davis, F. A., Maxfield, M. W., *Statistics Manual*, U. S. Naval Ordnance Test Station, China Lake, Calif., 1955

7. Forster, K. E., and Greif, R., "Heat Transfer to a Boiling Liquid; Mechanism and Correlations," Paper No. 58-HT-11, Second National Heat Transfer Conference, Chicago, Ill., Aug. 18-21, 1958

8. Gambill, W. R. and Greene, N. D., "A Preliminary Study of Boiling Burn-out Heat Fluxes for Water in Vortex Flow," Preprint 29, Second National Heat Transfer Conference, Chicago, Ill., Aug. 18-21, 1958

9. Griffith, Peter, and Wallis, John D., "The Role of Surface Conditions in Nucleate Boiling," *Chem. Eng. Progress Symposium Series*, No. 30, Vol. 56 (1960), p. 49-63

10. Gunther, F. C., and Kreith, F., "Photographic Study of Bubble Forma-
tion in Heat Transfer to Subcooled Water," Prog. Report No. 4-120,
Jet Prop. Lab., Calif. Inst. Tech., March, 1950

11. Harrison, W. B., and Levine, Z., "Wetting Effects on Boiling Heat
Transfer -- The Copper-Stearic Acid System," Paper No. 57-HT-29, ASME -
AIChE Joint Heat Transfer Conference, State College, Penn; Aug. 11-14,
1957

12. Hughmark, G. A., "A Statistical Analysis of Nucleate Pool Boiling
Data," AIChE National Meeting, Cleveland, Ohio, Abstract No. 41, 10
pages, May, 1961

13. Jakob, Max, Heat Transfer, Vol. 1, Wiley, 1949

14. McAdams, W. H., Heat Transmission, 3rd Ed., McGraw - Hill, 1954

15. Moore, F. D., and Mesler, R. B., "The Measurement of Rapid Surface
Temperature Fluctuations During Nucleate Boiling of Water," AIChE
Journal, 7, No. 4, p. 620-4 (Dec. 1961)

16. Nickelson, R. L., "Some Effects of Heat Transfer Surfaces Observed
in Natural Convection and Nucleate Pool Boiling Heat Transfer,"
PhD. Thesis, Dept. Chem. Eng., Univ. of Minn., Minneapolis, Minn.,
1957

17. Nukiyama, Shiro, "Maximum and Minimum Values of Heat Transmitted from
Metal to Boiling Water Under Atmospheric Pressure," J. Soc. Mech.
Eng. Japan, 37, No. 206, 367-374 (1934)

18. Ostle, Bernard, Statistics in Research, Iowa State College Press, Ames,
Iowa, 1954

19. Volk, William, Applied Statistics for Engineers, McGraw-Hill, New York,
1958

20. Westwater, J. W., "Boiling Heat Transfer," American Scientist, Vol. 47, No. 3, p. 427-46 (Sept. 1959)

21. Westwater, J. W., "Nucleate Pool Boiling," Petro/Chem Engineer, Vol. 32, No. 9, p. 40-3 (Aug. 1961)

22. Westwater, J. W., "Nucleate Pool Boiling," Petro/Chem Engineer, Vol. 33, No. 10, p. 53-60 (Sept. 1961)